NASA Contractor Report 189665
ICASE Report No. 92-24

ICASE

A COMPUTATIONAL ALGORITHM FOR CRACK DETERMINATION. THE MULTIPLE CRACK CASE

Kurt Bryan
Michael Vogelius

Contract Nos. NAS1-18605, NAS1-19480
June 1992

Institute for Computer Applications in Science and Engineering
NASA Langley Research Center
Hampton, Virginia 23665-5225

Operated by the Universities Space Research Association

National Aeronautics and
Space Administration

Langley Research Center
Hampton, Virginia 23665-5225

A COMPUTATIONAL ALGORITHM FOR CRACK DETERMINATION. THE MULTIPLE CRACK CASE [1]

Kurt Bryan
Institute for Computer Applications in Science and Engineering
NASA Langley Research Center
Hampton, VA 23665

Michael Vogelius
Department of Mathematics
Rutgers University
New Brunswick, N.J. 08903

Abstract

This paper develops an algorithm for recovering a collection of linear cracks in a homogeneous electrical conductor from boundary measurements of voltages induced by specified current fluxes. The technique is a variation of Newton's method and is based on taking weighted averages of the boundary data. The method also adaptively changes the applied current flux at each iteration to maintain maximum sensitivity to the estimated locations of the cracks.

[1]The first author is partially supported by National Aeronautics and Space Administration contracts NAS1-18605 and NAS1-19480; the second author is partially supported by National Science Foundation Grant DMS-89-02532 and AFOSR Contract 89-NM-605.

1 Introduction

In this paper we develop a very efficient computational algorithm to reconstruct a collection of linear cracks inside a homogeneous conductor from electrostatic boundary measurements. The algorithm in this paper can be seen as a natural extension of the algorithm developed in [15] for the reconstruction of a single crack. This extension poses several theoretical as well as practical challenges. We have also significantly improved the efficiency and versatility of the earlier algorithm by basing all computations for the underlying conductance problem on a one-dimensional boundary integral formulation instead of a two-dimensional finite element formulation. It should be mentioned here that boundary integral formulations have been used in other implementations of (single) crack reconstruction algorithms [13], [14], and also that progress on the development of an algorithm for the reconstruction of a single (penny-shaped) crack inside a three dimensional object is reported in [14]. Algorithms like the one discussed in this paper are significantly different from more general purpose imaging algorithms (*cf.* [3], [6], [9], [16]) that seek to reconstruct an unknown distributed conductivity profile from similar boundary measurements. Algorithms such as ours are based on the assumption that certain apriori information about the profile is available and they incorporate this knowledge into the reconstruction in such a way as to achieve better continuous dependence and better discrete approximation properties. One important feature of the present algorithm is that it is based on an adaptive change of the prescribed boundary current patterns to ensure "maximal" sensitivity. The idea to use some kind of "optimal" current pattern in connection with impedance imaging has been developed by Gisser, Isaacson and Newell (*cf.* [9]); the specific strategy we use is somewhat different from theirs and ties in directly with the iterative procedure (it does not rely on any eigenfunctions). Our reconstruction is based on the usage of relatively few averages of the boundary voltage measurements (as opposed to all the boundary voltage data). In addition to improving the efficiency of the algorithm, this should also decrease the probability of getting caught in a local minimum when compared to more standard output least-squares algorithms.

An outline of this paper is as follows. In Section 2 we present the "customary" mathematical model of electrostatic conductance for a smooth, isotropic background medium that

contains a collection of cracks. In particular we demonstrate the duality between the notions of perfectly insulating cracks and perfectly conducting cracks. We also briefly discuss known uniqueness and continuous dependence results. Section 3 contains a detailed description of the $4n$ functionals that we use for the reconstruction of a collection of n or fewer linear cracks. This section also provides a discussion of the adaptive strategy that we use for the selection of the "maximally sensitive" electrode locations. The boundary integral formulation of the electrostatic conductance problem and its discretization by Nyström's method is the topic of Section 4. The central part of the reconstruction algorithm is a version of Newton's method. This particular version together with the required gradient computation is discussed in Section 5. Section 6 contains a selection of representative computational experiments with our algorithm. Finally in Section 7 we provide a brief summary of our results and a description of possible future developments.

2 The Mathematical Model

A single crack is commonly modeled as a perfectly insulating curve σ. With a background conductivity $0 < \gamma_0 \leq \gamma(x) \leq \gamma_1$ and a finite collection of cracks $\Sigma = \cup_{k=1}^{n} \sigma_k$, the steady state conductance equations thus read

$$\begin{aligned} \nabla \cdot (\gamma \nabla v) &= 0 \quad \text{in} \quad \Omega \setminus \Sigma, \\ \gamma \frac{\partial v}{\partial \nu} &= 0 \quad \text{on} \quad \Sigma, \end{aligned} \tag{2.1}$$

with appropriate boundary conditions on $\partial\Omega$, *e.g.*,

$$v = \phi \quad \text{on} \quad \partial\Omega. \tag{2.2}$$

The field ν is normal to Σ. The function v represents the voltage potential induced in Ω. We assume that Ω is simply connected, *i.e.*, it has no holes, and so the entire boundary $\partial\Omega$ is accessible from the "outside". Let u denote the "γ-harmonic" conjugate to v. It is related to v by the formula

$$(\nabla u)^{\perp} = \gamma \nabla v, \tag{2.3}$$

where $\perp$ indicates counter-clockwise rotation by $\pi/2$. For a particular set of constants c_k, $k = 1, \ldots, n$, the function u solves the problem

$$\begin{aligned} \nabla \cdot (\gamma^{-1} \nabla u) &= 0 \quad \text{in} \quad \Omega \setminus \Sigma, \\ u &= c_k \quad \text{on} \quad \sigma_k, \; k = 1, \ldots, n \end{aligned} \tag{2.4}$$

with

$$\gamma^{-1} \frac{\partial u}{\partial \nu} = \psi = \frac{\partial \phi}{\partial s} \text{ on } \partial\Omega. \tag{2.5}$$

Here s denotes the counter-clockwise tangent direction on $\partial\Omega$ and ν denotes the outward normal on $\partial\Omega$. For these particular constants, finding a solution to (2.1), (2.2) is thus equivalent to finding a solution to (2.4), (2.5). The constants c_k may (up to a common additive constant) be characterized in several equivalent ways:

(a) Let A be the $n \times n$-matrix with elements $A_{ij} = \int_\Omega \gamma^{-1} \nabla U^{(i)} \nabla U^{(j)} dx$ and let b be the n-vector with elements $b_i = \int_{\partial\Omega} \psi U^{(i)} ds$, where $U^{(j)}$, $j = 1, \ldots, n$, denote the solutions to

$$\begin{aligned} \nabla \cdot (\gamma^{-1} \nabla U^{(j)}) &= 0 \quad \text{in} \quad \Omega \setminus \Sigma, \\ U^{(j)} &= 1 \quad \text{on} \quad \sigma_j, \\ U^{(j)} &= 0 \quad \text{on} \quad \sigma_k, \; k \neq j \end{aligned}$$

with

$$\gamma^{-1} \frac{\partial U^{(j)}}{\partial \nu} = 0 \quad \text{on} \quad \partial\Omega.$$

Then the vector $c = (c_1, \ldots, c_n)^t$ is the solution to $Ac = b$.

(b) The "γ-harmonic" conjugate, u, satisfies $\int_{\sigma_k} [\gamma^{-1} \frac{\partial u}{\partial \nu}] \, ds = 0$, $1 \leq k \leq n$. Here $[\gamma^{-1} \frac{\partial u}{\partial \nu}] = \gamma^{-1} \frac{\partial u}{\partial \nu_-} - \gamma^{-1} \frac{\partial u}{\partial \nu_+}$ denotes the jump in the normal flux across the curve σ_k. [2] Furthermore, the set of constants $\{c_k\}_{k=1}^n$ is the unique set of constants for which the solution to (2.4), (2.5) has this property.

[2] The expression $\frac{\partial u}{\partial \nu_+}$ denotes the limit of the derivative (in the direction ν) as one approaches σ_k from the side to which ν points. $\frac{\partial u}{\partial \nu_-}$ denotes the limit as one approaches σ_k from the opposite side.

(c) Let T be a fixed point on $\partial\Omega$, in a neighborhood of which ϕ is smooth. Let τ_k be a smooth curve in $\Omega \setminus \Sigma$ connecting T to an interior point of the crack σ_k, and let s denote the unit tangent direction along τ_k, pointing from T towards σ_k. Then the constants c_k are given by the formulae

$$c_k = -\int_{\tau_k} \gamma \frac{\partial v}{\partial \nu}\, ds + u(T),$$

where ν denotes the normal field $\nu = -s^{\perp}$.

The characterization (c) is a direct consequence of the relation (2.3). The characterizations (a) and (b) are practically much more useful; they are both a consequence of the following well known result from convex duality.

Proposition 2.1 *If ϕ is an element of $H^{1/2}(\partial\Omega)$, then the field $\xi = \gamma\nabla v$ is the (unique) minimizer of the functional*

$$\frac{1}{2}\int_{\Omega} \gamma^{-1}|\eta|^2\, dx - \int_{\partial\Omega} \phi\, \eta\cdot\nu\, ds \tag{2.6}$$

in the space $H = L^2(\Omega) \cap \{\eta : \nabla\cdot\eta = 0 \ \text{ in } \ \Omega\setminus\Sigma\ ,\ \eta\cdot\nu = 0 \text{ on } \sigma_k,\ \ k{=}1,\ldots,n\}$.

It is not difficult to see that any element of the space H satisfies $\nabla\cdot\eta = 0$ in *all* of Ω and therefore has the form $\eta = (\nabla w)^{\perp}$ for some $w \in H^1(\Omega)$, with w being constant on each σ_k. Conversely, it is also true that any vector field of the form $\eta = (\nabla w)^{\perp}$, $w \in H^1(\Omega) \cap\{w = \text{constant on each } \sigma_k,\ k = 1, \ldots, n\}$, is in the space H. After insertion into (2.6) we obtain $\gamma\nabla v = (\nabla u)^{\perp}$, where u is the minimizer of the functional

$$\frac{1}{2}\int_{\Omega} \gamma^{-1}|\nabla w|^2\, dx - \int_{\partial\Omega} \frac{\partial\phi}{\partial s} w\, ds$$

in the space $H^1(\Omega)\cap\{w = \text{constant on each } \sigma_k,\ k = 1, \ldots, n\}$. This provides a variational characterization of the "γ-harmonic" conjugate to v. Let $F(d)$, $d \in \mathbb{R}^n$, denote the expression

$$F(d) = \frac{1}{2}\int_{\Omega} \gamma^{-1}|\nabla(u + \sum_{k=1}^{n} d_k U^{(k)})|^2\, dx - \int_{\partial\Omega} \psi(u + \sum_{k=1}^{n} d_k U^{(k)})\, ds.$$

From the above discussion it is clear that the set of constants corresponding to u are characterized by the fact that $d = 0$ is a minimum of F. Equivalently (because of the form of

F), the set of constants corresponding to u are characterized by the fact that $d = 0$ is a stationary point for F. Stationarity of $d = 0$ is equivalent to the conditions

$$\int_\Omega \gamma^{-1} \nabla u \nabla U^{(k)} \, dx = \int_{\partial\Omega} \psi U^{(k)} \, ds, \quad k = 1, \ \ldots, n. \tag{2.7}$$

From integration by parts (on the domain $\Omega \setminus \Sigma$) we have

$$\int_\Omega \gamma^{-1} \nabla u \nabla U^{(k)} \, dx = \int_{\sigma_k} [\gamma^{-1} \frac{\partial u}{\partial \nu}] \, ds + \int_{\partial\Omega} \psi U^{(k)} \, ds.$$

Insertion of this into (2.7) now gives that the set of constants corresponding to u are characterized by

$$\int_{\sigma_k} [\gamma^{-1} \frac{\partial u}{\partial \nu}] \, ds = 0 \quad k = 1, \ \ldots, n,$$

as asserted in (b).

On the other hand, the function u has the form

$$u = u_0 + \sum_{i=1}^{n} c_i U^{(i)}, \tag{2.8}$$

where u_0 is the solution to

$$\begin{aligned} \nabla \cdot (\gamma^{-1} \nabla u_0) &= 0 \quad \text{in} \quad \Omega \setminus \Sigma, \\ u_0 &= 0 \quad \text{on} \quad \sigma_k, \ k = 1, \ldots, n, \end{aligned} \tag{2.9}$$

with

$$\gamma^{-1} \frac{\partial u_0}{\partial \nu} = \psi \quad \text{on} \quad \partial\Omega. \tag{2.10}$$

Because of (2.9) and (2.10) we have $\int_\Omega \gamma^{-1} \nabla u_0 \nabla U^{(k)} \, dx = 0$; by insertion of (2.8) into (2.7) and use of this formula we now obtain

$$\sum_{i=1}^{n} c_i \int_\Omega \gamma^{-1} \nabla U^{(i)} \nabla U^{(k)} \, dx = \int_{\partial\Omega} \psi U^{(k)} \, ds \quad k = 1, \ldots, n,$$

which is exactly the characterization (a). The above argument rests on the fact that ϕ is in $H^{1/2}(\partial\Omega)$ (ψ is in $H^{-1/2}(\partial\Omega)$). However, by continuity the characterizations carry over to cases in which ϕ (and ψ) are not necessarily so regular that u is a variational solution. In particular these characterizations remain valid if ψ consists of delta functions, a type of boundary current we shall repeatedly use in this paper.

Since u and v are related by the equation $(\nabla u)^{\perp} = \gamma \nabla v$, it is clear that knowledge of the pair $(\phi, \gamma \frac{\partial v}{\partial \nu}|_{\partial\Omega})$ is equivalent to knowledge of the pair $(u|_{\partial\Omega}, \psi)$. It is much more convenient to work with the function u as opposed to the function v, and we shall entirely do so for the development of our algorithm. In particular by working with u we avoid the difficulties that are associated with non integrable kernels in the integral equation formulation (*cf.* [12], [14]).

Let $P_0, \ \ldots \ , P_M$ be $M+1$ points on $\partial\Omega$; we assume that these points are labeled in order of counter-clockwise appearance, starting from P_0. For the crack reconstruction we utilize solutions corresponding to the two-electrode currents $\psi_j = \delta_{P_0} - \delta_{P_j}$, $j = 1, \ldots, M$,

$$\begin{aligned} \nabla \cdot (\gamma^{-1} \nabla u_j) &= 0 \quad \text{in} \quad \Omega \setminus \Sigma, \\ u_j &= c_k^{(j)} \quad \text{on} \quad \sigma_k, \ k = 1, \ \ldots \ , n, \end{aligned} \tag{2.11}$$

with

$$\gamma^{-1} \frac{\partial u_j}{\partial \nu} = \delta_{P_0} - \delta_{P_j} \quad \text{on} \quad \partial\Omega, \tag{2.12}$$

the constants $c_k^{(j)}$ being selected so that $\int_{\sigma_k} [\gamma^{-1} \frac{\partial u_j}{\partial \nu}] \, ds = 0$ for $k = 1, \ \ldots \ , n$. The inverse problem may now be stated explicitly as follows:

We seek to reconstruct the collection of cracks $\Sigma = \cup_{k=1}^{n} \sigma_k$ *from knowledge of the boundary voltage data* $\{u_j|_{\partial\Omega}\}_{j=1}^{M}$ *corresponding to the prescribed two-electrode currents* $\gamma^{-1} \frac{\partial u_j}{\partial \nu} = \delta_{P_0} - \delta_{P_j}$, $j = 1, \ \ldots \ , M$.

It is known that boundary voltage measurements corresponding to $M = n + 1$ fixed two-electrode currents suffice to uniquely identify a collection of n (or fewer) cracks [4]. This result is an extension of a result in [8] which asserts that boundary voltage measurements corresponding to two fixed two-electrode currents suffice to uniquely identify a single crack. Recently an interesting continuous dependence estimate has been obtained for the case when the background conductivity is constant and there is at most one crack [1]. Briefly described, this estimate states that if the boundary voltage data (on some open subset of $\partial\Omega$) deviate by ϵ then the crack locations differ by at most $[\log(|\log \epsilon|)]^{-1/4}$. In the present paper shall always try to fit the data entirely by means of linear cracks. For such cracks one can hope to have better continuous dependence estimates, as indicated by the results in [8]. As was the case in [15], we base the reconstruction of the cracks on the values of a number

of functionals (as opposed to all the boundary voltage measurements). In [15] we used 4 functionals corresponding to the reconstruction of a single linear crack; the natural extension is to use $4n$ functionals for the reconstruction of n cracks. In the following section we give a careful description of these functionals.

3 The Functionals

We now specialize to the case of a constant background conductivity, $\gamma \equiv 1$. Let $\mathbf{F}$ denote the vector-valued function

$$\mathbf{F}(\Sigma, \psi, \mathbf{w}) = (F(\Sigma, \psi, w^{(1)}), F(\Sigma, \psi, w^{(2)}), F(\Sigma, \psi, w^{(3)}), F(\Sigma, \psi, w^{(4)}))^t,$$

where $F(\Sigma, \psi, w)$ is given by

$$F(\Sigma, \psi, w) = \int_{\partial\Omega} u(\Sigma, \psi) \frac{\partial w}{\partial \nu}\, ds, \tag{3.1}$$

and where $w^{(i)}$, $1 \leq i \leq 4$, are particular solutions of

$$\triangle w = 0 \quad \text{in} \quad \mathbb{R}^2 \setminus \Sigma.$$

The function $u = u(\Sigma, \psi)$ is the solution to

$$\begin{aligned} \triangle u &= 0 \text{ in } \Omega \setminus \Sigma, \\ u &= c_k \text{ on } \sigma_k, \quad k = 1, \ldots, n, \\ \frac{\partial u}{\partial \nu} &= \psi \text{ on } \partial\Omega, \end{aligned} \tag{3.2}$$

with the constants c_k uniquely specified by

$$\int_{\partial\Omega} u\, ds = 0 \quad \text{and} \quad \int_{\sigma_k} \left[\frac{\partial u}{\partial \nu}\right] ds = 0, \quad k = 1, \ldots, n.$$

The exact selection of boundary currents ψ and test functions $\mathbf{w} = (w^{(1)}, w^{(2)}, w^{(3)}, w^{(4)})^t$ is very important and will be discussed shortly. We select one ψ and one $\mathbf{w}$ corresponding to each crack σ_k; whenever we want to emphasize this correspondence we use the notation

$$\psi_{\sigma_k} \quad \text{and} \quad \mathbf{w}_{\sigma_k} = (w^{(1)}_{\sigma_k}, w^{(2)}_{\sigma_k}, w^{(3)}_{\sigma_k}, w^{(4)}_{\sigma_k})^t.$$

We have for convenience chosen the normalization $\int_{\partial\Omega} u\, ds = 0$ for the voltage potential. We shall always select $\mathbf{w}$ so that

$$\int_{\partial\Omega} \frac{\partial w^{(i)}}{\partial \nu}\, ds = 0, \quad \text{and} \quad \int_{\sigma_k} \left[\frac{\partial w^{(i)}}{\partial \nu}\right] ds = 0 \quad k = 1, \ldots, n. \tag{3.3}$$

Because of the first identity in (3.3) the function $\mathbf{F}$ is unchanged by the addition of a constant to u, and we could therefore just as easily work with any other normalization. The components of $\mathbf{F}$ are just weighted averages of the boundary voltage data. We use a weighting function of the form $\frac{\partial w}{\partial \nu}$ because of the relation

$$\int_{\partial\Omega} u(\Sigma, \psi) \frac{\partial w}{\partial \nu}\, ds = \int_{\Omega \setminus \Sigma} \nabla u(\Sigma, \psi) \nabla w\, dx \tag{3.4}$$

that exists between the expression in equation (3.1) and the energy bilinear form (by means of Green's formula). As will be seen later, these averages are equivalent, in the absence of any crack, to the set of the first 4 nontrivial Fourier modes of the induced boundary voltage.

The data for our reconstruction consist of measured boundary potentials corresponding to certain prescribed two-electrode boundary currents. We denote the voltage data corresponding to the boundary current ψ by $g(\psi)$ and define a corresponding vector-valued function

$$\mathbf{f}\ (\psi, \mathbf{w}) = (f(\psi, w^{(1)}), f(\psi, w^{(2)}), f(\psi, w^{(3)}), f(\psi, w^{(4)}))^t,$$

where $f(\psi, w)$ is given by

$$f(\psi, w) = \int_{\partial\Omega} g(\psi) \frac{\partial w}{\partial \nu}\, ds,$$

and where $w^{(i)}$ are the same functions as before. Our algorithm seeks a solution $\Sigma = \{\sigma_k\}_{k=1}^n$ to the $4n$ equations

$$\mathbf{F}(\Sigma, \psi_{\sigma_k}, \mathbf{w}_{\sigma_k}) = \mathbf{f}\ (\psi_{\sigma_k}, \mathbf{w}_{\sigma_k}), \quad 1 \le k \le n.$$

Consequently, we do not use information about the full boundary voltages for the reconstruction; we only use information about the values of these particular functionals.

We implicitly assume that our data is consistent so that $\mathbf{f}\ (\psi_{\sigma_k}, \mathbf{w}_{\sigma_k})$ corresponds to some collection of cracks Σ^* (Σ^* may consist of fewer than n cracks). In reality we therefore solve

$$\mathbf{G}_k(\Sigma) = 0, \quad 1 \le k \le n, \tag{3.5}$$

with

$$\begin{aligned} \mathbf{G}_k(\Sigma) &= \mathbf{F}(\Sigma, \psi_{\sigma_k}, \mathbf{w}_{\sigma_k}) - \mathbf{F}(\Sigma^*, \psi_{\sigma_k}, \mathbf{w}_{\sigma_k}) \\ &= \mathbf{F}(\Sigma, \psi_{\sigma_k}, \mathbf{w}_{\sigma_k}) - \mathbf{f}\ (\psi_{\sigma_k}, \mathbf{w}_{\sigma_k}). \end{aligned} \tag{3.6}$$

Clearly Σ^* is a solution to (3.5). If the Frechet derivative $D_\Sigma\{\mathbf{G}_k\}|_{\Sigma=\Sigma^*}$ (a $4n \times 4n$ matrix) is nonsingular, then Σ^* is indeed the unique solution to (3.5) near Σ^*, and furthermore, one may expect that some variation of Newton's method will be an efficient solution technique. Differentiation with application of the "chain rule" yields the expression

$$D_\Sigma\{\mathbf{G}_k\}_{k=1}^n|_{\Sigma=\Sigma^*} = \{D_\Sigma \mathbf{F}(\Sigma, \psi_{\sigma_k^*}, \mathbf{w}_{\sigma_k^*})|_{\Sigma=\Sigma^*}\}_{k=1}^n,$$

for the derivative with respect to Σ (at Σ^*), the right hand side of which is a $4n \times 4n$ matrix with rows

$$D_\Sigma F(\Sigma, \psi_{\sigma_k^*}, w_{\sigma_k^*}^{(i)})|_{\Sigma=\Sigma^*} = \int_{\partial\Omega} D_\Sigma u(\Sigma, \psi_{\sigma_k^*})|_{\Sigma=\Sigma^*} \frac{\partial w_{\sigma_k^*}^{(i)}}{\partial \nu}\, ds, \tag{3.7}$$
$$1 \le k \le n,\ 1 \le i \le 4.$$

In [15] we explicitly calculated the expression (3.7) in terms of u and $\frac{\partial u}{\partial \nu}$ (eliminating $D_\Sigma u$); we used this alternate expression for the selection of the "maximally sensitive two-electrode" currents as well as for the Newton's update itself. In our implementation here we shall rely on essentially the same technique as in [15] for the selection of two-electrode currents, but we shall directly compute the derivative of $u(\Sigma, \psi)$ with respect to Σ at the discrete level (*cf.* Section 5) for use with the Newton's update.

When talking about the derivative with respect to Σ, we mean the derivative with respect to the $4n$ parameters that are used to describe Σ. Just as in [15] we parametrize a single crack by (b_1, b_2), θ, and λ, where (b_1, b_2) are the coordinates of one endpoint, θ is the counter-clockwise angle between the crack and the halfline $y = b_2$, $x > b_1$, and λ is the length of the crack (here coordinates of points are relative to a fixed reference coordinate system). For convenience we order these coordinates $\mathbf{q} = (\theta, b_2, b_1, \lambda)$; the parameter set corresponding to Σ is now given by the vector $\mathbf{Q} = (\mathbf{q}_1, \mathbf{q}_2, \ \ldots\ , \mathbf{q}_n)^t$. The derivative $D_\Sigma\{\mathbf{G}_k\}$ consists of the (n^2) 4×4 blocks

$$D_{\mathbf{q}_l}\mathbf{G}_k.$$

At the solution, $\Sigma = \Sigma^*$, these blocks equal

$$D_{\mathbf{q}_l}\mathbf{F}(\mathbf{Q}, \psi_{\sigma_k^*}, \mathbf{w}_{\sigma_k^*})|_{\mathbf{Q}=\mathbf{Q}^*}. \tag{3.8}$$

If the derivatives (3.8) are formed at some $\mathbf{Q}^0$ not equal to $\mathbf{Q}^*$ then they no longer represent the full derivative of $\{\mathbf{G}_k\}$; the latter also includes terms where $\mathbf{w}_{\sigma_k}$ and ψ_{σ_k} are differentiated through (*cf.* (3.6)). For the Newton's update we use a more complete "derivative" which includes the terms that arise when the $\mathbf{w}_{\sigma_k}$ are differentiated through, but we do not include differentiation through ψ_{σ_k}. The goal behind the choice of $\mathbf{w}_{\sigma_k}$ and ψ_{σ_k} is to make the derivative of $\{\mathbf{G}_k\}$ as far from singular as possible at $\Sigma = \Sigma^0$, the current stage of the iteration.

In order to describe the choice of $\mathbf{w}_{\sigma_k}$ we select a coordinate system such that σ_k lies on the positive x_1 axis, with one endpoint at the origin. In this coordinate system we choose

$$w_{\sigma_k}^{(1)} = \mathrm{Im}[z], \quad w_{\sigma_k}^{(2)} = \mathrm{Im}[z^2], \tag{3.9}$$

$$w_{\sigma_k}^{(3)} = \begin{cases} \mathrm{Re}[(z-\lambda_k)\sqrt{z(z-\lambda_k)}], & Re(z) > \frac{\lambda_k}{2} \\ -\mathrm{Re}[(z-\lambda_k)\sqrt{z(z-\lambda_k)}], & Re(z) < \frac{\lambda_k}{2} \end{cases} \tag{3.10}$$

$$w_{\sigma_k}^{(4)} = \begin{cases} \mathrm{Re}[\sqrt{z(z-\lambda_k)}], & Re(z) > \frac{\lambda_k}{2} \\ -\mathrm{Re}[\sqrt{z(z-\lambda_k)}], & Re(z) < \frac{\lambda_k}{2} \end{cases} \tag{3.11}$$

where $z = x_1 + ix_2$ and λ_k denotes the length of σ_k. The functions $w_{\sigma_k}^{(3)}$ and $w_{\sigma_k}^{(4)}$ are extended to $\mathrm{Re}(z) = \lambda_k/2$ by continuity. Except for a change in $w_{\sigma_k}^{(4)}$, this is exactly the same choice of test functions as in [15]. Since they are harmonic in Ω, the two functions $w_{\sigma_k}^{(1)}$ and $w_{\sigma_k}^{(2)}$ clearly satisfy (3.3). It requires some extra calculations to check that $w_{\sigma_k}^{(3)}$ and $w_{\sigma_k}^{(4)}$ also satisfy (3.3); for reasons of brevity we omit these calculations here. The fact that $w_{\sigma_k}^{(3)}$ and $w_{\sigma_k}^{(4)}$ do indeed satisfy (3.3) makes the Remark 1 in Section 3 of [15] superfluous. Notice that $w_{\sigma_k}^{(i)}$, $1 \le i \le 4$, vanish on the crack σ_k.

Remark

Given the specific form of the weight functions $w_{\sigma_k}^{(i)}$ it is now fairly easy to explain why, in the definition of $\mathbf{G}_k$, we pick a distinct boundary current ψ_{σ_k} corresponding to each k. If as

an extreme we had picked the same boundary current ψ corresponding to each crack, then the first two equations of (3.5), (3.6) would be solved *for all* k if

$$\begin{aligned}
\int_{\partial\Omega} \frac{\partial}{\partial\nu}(x) u(\Sigma,\psi)\, ds &= \int_{\partial\Omega} \frac{\partial}{\partial\nu}(x) g(\psi)\, ds, \\
\int_{\partial\Omega} \frac{\partial}{\partial\nu}(y) u(\Sigma,\psi)\, ds &= \int_{\partial\Omega} \frac{\partial}{\partial\nu}(y) g(\psi)\, ds, \\
\int_{\partial\Omega} \frac{\partial}{\partial\nu}(x^2-y^2) u(\Sigma,\psi)\, ds &= \int_{\partial\Omega} \frac{\partial}{\partial\nu}(x^2-y^2) g(\psi)\, ds \\
\int_{\partial\Omega} \frac{\partial}{\partial\nu}(xy) u(\Sigma,\psi)\, ds &= \int_{\partial\Omega} \frac{\partial}{\partial\nu}(xy) g(\psi)\, ds,
\end{aligned}$$

where (x, y) denote coordinates relative to some fixed coordinate system. The system (3.5), (3.6) would therefore represent no more than $2n + 4$ equations for the $4n$ unknowns of Σ. For $n > 2$ this immediately leads to "underdetermination" and a singular Jacobian. ■

In [15] we analyzed the structure of the derivative

$$D_{\mathbf{q}}\mathbf{F}(\mathbf{q}, \psi_{\sigma^0}, \mathbf{w}_{\sigma^0})|_{\mathbf{q}=\mathbf{q}^0}, \tag{3.12}$$

for the case of a single crack (and with a slightly different choice of $w^{(4)}_{\sigma_k}$). With the ordering of the parameters $(\theta, b_2, b_1, \lambda)$ we found that this 4×4 matrix was lower triangular. We also found that if the test functions $w^{(i)}$, $1 \le i \le 4$, had been selected harmonic (and 0 on the crack) then the last two columns in this matrix would have been zero. Test functions with singularities like $w^{(3)}$ and $w^{(4)}$ are thus essential to insure that this matrix is non-singular. Since the only change we make in the test functions concern $w^{(4)}$ we do not destroy the lower triangular structure of this derivative for the one crack case. In the multiple crack case the counterparts of the matrix just discussed are the diagonal entries

$$D_{\mathbf{q}_k}\mathbf{F}(\mathbf{Q}, \psi_{\sigma^0_k}, \mathbf{w}_{\sigma^0_k})|_{\mathbf{Q}=\mathbf{Q}^0}.$$

It is worthwhile noticing that these matrices *do not* inherit the lower triangular structure. For a any fixed crack σ_k contributions corresponding to the other cracks will appear above the diagonal. These contributions are of the form $-\int_{\sigma_l}[\frac{\partial u}{\partial\nu}]w^{(i)}_{\sigma_k,j}\, ds$, where the functions $w^{(i)}_{\sigma_k,j}$ are related to $w^{(i)}_{\sigma_k}$ by the formulae

$$\begin{aligned}
w^{(i)}_{\sigma_k,1} &= (-x_2, x_1)^t \cdot \nabla w^{(i)}_{\sigma_k}, \quad w^{(i)}_{\sigma_k,2} = \frac{\partial w^{(i)}_{\sigma_k}}{\partial x_2}, \\
w^{(i)}_{\sigma_k,3} &= \frac{\partial w^{(i)}_{\sigma_k}}{\partial x_1}, \quad w^{(i)}_{\sigma_k,4} = (x_1, x_2)^t \cdot \nabla w^{(i)}_{\sigma_k},
\end{aligned} \tag{3.13}$$

cf. [15], page 921. However, it is our practical experience that the above selection of $w_{\sigma_k}^{(i)}$ together with the appropriate selection of the two-electrode current ψ_{σ_k} (to be discussed below) is a very effective way of achieving a Fréchet derivative which is far from singular.

Remark

It is interesting to consider the limit $\lambda_k \to 0$ as one endpoint and the direction of the crack stay fixed. Let σ_k be a crack with endpoint at (b_1, b_2), zero angle, and length λ_k. The corresponding limits of the functions $w_{\sigma_k}^{(i)}$ are given in absolute coordinates by

$$\begin{aligned} w_0^{(1)} &= y - b_2, \qquad w_0^{(2)} = 2(x - b_1)(y - b_2), \\ w_0^{(3)} &= (x - b_1)^2 - (y - b_2)^2, \qquad w_0^{(4)} = x - b_1. \end{aligned} \tag{3.14}$$

Actually, $w_{\sigma_k}^{(1)} = w_0^{(1)}$ and $w_{\sigma_k}^{(2)} = w_0^{(2)}$ identically, since these two functions do not depend on the crack length. Moreover, the approximations $w_{\sigma_k}^{(3)} \approx w_0^{(3)}$ and $w_{\sigma_k}^{(4)} \approx w_0^{(4)}$ for the third and fourth functionals are quite accurate sufficiently far away (e.g. two crack lengths) from the crack. If Ω is the unit ball and $g(\theta)$, $0 \le \theta \le 2\pi$, is the limiting boundary voltage, and $F_i^0 = \lim_{\lambda_k \to 0} F(\Sigma, \psi, w_{\sigma_k}^{(i)})$, then (3.14) gives

$$\begin{aligned} F_1^0 &= \textstyle\int_0^{2\pi} g(\theta) \sin\theta \; d\theta \\ F_2^0 &= 2\textstyle\int_0^{2\pi} g(\theta) \sin 2\theta \; d\theta - 2b_1 \int_0^{2\pi} g(\theta) \sin\theta \; d\theta - 2b_2 \int_0^{2\pi} g(\theta) \cos\theta \; d\theta \\ F_3^0 &= 2\textstyle\int_0^{2\pi} g(\theta) \cos 2\theta \; d\theta - 2b_1 \int_0^{2\pi} g(\theta) \cos\theta \; d\theta + 2b_2 \int_0^{2\pi} g(\theta) \sin\theta \; d\theta \\ F_4^0 &= \textstyle\int_0^{2\pi} g(\theta) \cos\theta \; d\theta. \end{aligned}$$

In the limit $\lambda_k \to 0$, $\mathbf{F}$ thus represents the first 4 Fourier modes of the boundary data. ■

The change we have made in $w^{(4)}$ can be explained from this remark: with the choice made in [15] $w^{(3)}$ and $w^{(4)}$ had the same limit as $\lambda \to 0$. The boundary integral implementation of the algorithm would therefore occasionally attempt to fit the data by just making the cracks very small, since it then in effect only would have to satisfy $3n$ equations (using $3n$ unknowns) as opposed to satisfying a larger set of $4n$ equations. We did not encounter this phenomenon in any of the single crack experiments performed in [15] since the implementation there was based on a 2-d finite element formulation, which effectively put a lower bound on the crack length. The new $w^{(4)}$ we have introduced here is simply a (correctly scaled) linear combination of the $w^{(4)}$ and $w^{(3)}$ used in [15].

For the selection of the current ψ_{σ_k} we rely on an appropriate adaptation of the technique developed in [15]. In that paper we calculated that the first and second diagonal entries of the matrix (3.12) are m and $2m$ respectively, where m denotes the expression

$$m = \int_{\partial\Omega} \left(u \frac{\partial w_1^{(1)}}{\partial \nu} - \psi w_1^{(1)} \right) \, ds.$$

We then proceeded to select a two-electrode current which made this expression largest possible. In the multiple crack case the first diagonal entry of the k'th diagonal block of $\{D_\Sigma \mathbf{F}(\Sigma, \psi_{\sigma_k}, \mathbf{w}_{\sigma_k})\}_{k=1}^n$ is given by

$$m_k = \int_{\partial\Omega} \left(u \frac{\partial w_{\sigma_k,1}^{(1)}}{\partial \nu} - \psi w_{\sigma_k,1}^{(1)} \right) \, ds - \Sigma_{l \neq k} \int_{\sigma_l} \left[\frac{\partial u}{\partial \nu} \right] w_{\sigma_k,1}^{(1)} \, ds \ , \tag{3.15}$$

where $w_{\sigma_k,1}^{(1)}$ is as defined by (3.13).

Consider the function $\xi_k \in H^1(\Omega \setminus \sigma_k)$ satisfying

$$\begin{aligned} \triangle \xi_k &= 0 \quad \text{in} \quad \Omega \setminus \sigma_k, \\ \xi_k &= 0 \quad \text{on} \quad \sigma_k, \\ \frac{\partial \xi_k}{\partial \nu} &= \frac{\partial w_{\sigma_k,1}^{(1)}}{\partial \nu} \quad \text{on} \quad \partial\Omega. \end{aligned} \tag{3.16}$$

Note that $w_{\sigma_k,1}^{(1)}$ does not identically vanish on σ_k, so that ξ_k is different from $w_{\sigma_k,1}^{(1)}$. After insertion of ξ_k into (3.15) we have

$$\begin{aligned} m_k &= \int_{\partial\Omega} \left(u \frac{\partial \xi_k}{\partial \nu} - \psi w_{\sigma_k,1}^{(1)} \right) \, ds - \Sigma_{l \neq k} \int_{\sigma_l} \left[\frac{\partial u}{\partial \nu} \right] w_{\sigma_k,1}^{(1)} \, ds \\ &= \int_{\partial\Omega} \psi (\xi_k - w_{\sigma_k,1}^{(1)}) \, ds + \int_{\sigma_k} \left([\frac{\partial u}{\partial \nu}] \xi_k - u [\frac{\partial \xi_k}{\partial \nu}] \right) \, ds \\ &\quad + \Sigma_{l \neq k} \int_{\sigma_l} [\frac{\partial u}{\partial \nu}] \left(\xi_k - w_{\sigma_k,1}^{(1)} \right) \, ds \\ &= \int_{\partial\Omega} \psi (\xi_k - w_{\sigma_k,1}^{(1)}) \, ds + \Sigma_{l \neq k} \int_{\sigma_l} [\frac{\partial u}{\partial \nu}] \left(\xi_k - w_{\sigma_k,1}^{(1)} \right) \, ds. \end{aligned} \tag{3.17}$$

To obtain the last identity we have used the fact that $\xi_k = 0$ on σ_k and that

$$\int_{\sigma_k} [\frac{\partial \xi_k}{\partial \nu}] \, ds = - \int_{\partial\Omega} \frac{\partial \xi_k}{\partial \nu} \, ds = - \int_{\partial\Omega} \frac{\partial w_{\sigma_k,1}^{(1)}}{\partial \nu} \, ds = 0.$$

Concerning the two terms in the last expression of equation (3.17), it is reasonable to assume that the first term $\int_{\partial\Omega} \psi (\xi_k - w_{\sigma_k,1}^{(1)}) \, ds$ will be the larger (at least for moderate size cracks).

If we now substitute $\psi = \delta_P - \delta_Q$ into the last expression in (3.17) and disregard the second term we get

$$m_k \approx (\xi_k - w^{(1)}_{\sigma_k,1})(P) - (\xi_k - w^{(1)}_{\sigma_k,1})(Q). \tag{3.18}$$

We now chose $\psi_{\sigma_1} = \delta_{P_0} - \delta_{P_1}$ so that P_0 maximizes $(\xi_1 - w^{(1)}_{\sigma_1,1})(P)$ and P_1 minimizes $(\xi_1 - w^{(1)}_{\sigma_1,1})(Q)$. For subsequent $2 \leq k \leq n$ we chose $\psi_{\sigma_k} = \delta_{P_0} - \delta_{P_k}$ (the same P_0 as for $k = 1$) where P_k is selected so that the expression $(\xi_k - w^{(1)}_{\sigma_k,1})(P_0) - (\xi_k - w^{(1)}_{\sigma_k,1})(P_k)$ is of maximal magnitude, subject to the constraint that the points $P_0, P_1, P_2, \ldots, P_n$ stay well separated. We cannot allow any of the P_j to coincide, for then we would be duplicating boundary measurements, potentially leading to a singular Jacobian as described in the remark before. The above construction makes the two-electrode currents appear somewhat like the currents used for the uniqueness result proven in [4]. For the uniqueness result we needed $n + 1$ two-electrode currents with $n+2$ distinct electrode locations – the currents prescribed above only number n (with $n + 1$ electrode locations). We expect that this deficiency is more than compensated by the fact that the electrode locations change as the iterations proceed.

4 Integral Equation Formulation and Discretization

We now proceed to formulate the boundary value problem (3.2) as an integral equation on the boundary of the region $\Omega \setminus \Sigma$. Let $\Gamma(x, y)$ denote the fundamental solution for the two dimensional Laplacian given by

$$\Gamma(x, y) = \frac{1}{2\pi} \log(|x - y|), \quad x, y \in \mathbb{R}^2.$$

The application of standard potential theory arguments (see [7], Sections 3.B-3.D) shows that u, the solution to (3.2), for $x \in \Omega \setminus \Sigma$, can be represented as

$$u(x) = \int_{\partial\Omega} (u(y) \frac{\partial}{\partial \nu_y} \Gamma(x, y) - \Gamma(x, y)\psi(y))\, ds_y - \sum_{k=1}^{n} \int_{\sigma_k} \Gamma(x, y) \left[\frac{\partial u}{\partial \nu}\right](y)\, ds_y. \tag{4.1}$$

Here $\frac{\partial}{\partial \nu_y}$ on $\partial\Omega$ denotes the normal outward derivative with respect to the y variable. On any of the cracks σ_k, ν denotes a unit normal field and $\left[\frac{\partial u}{\partial \nu}\right] = \frac{\partial u}{\partial \nu_-} - \frac{\partial u}{\partial \nu_+}$ denotes the jump in the normal flux across the crack. To simplify notation we shall use the notation ϕ_k for

the jump $\left[\frac{\partial u}{\partial \nu}\right]$ across σ_k. The formula (4.1) expresses the value of u at any point in $\Omega \setminus \Sigma$ in terms of the Dirichlet and Neumann data for u on $\partial\Omega$ and the jump in $\frac{\partial u}{\partial \nu}$ across the cracks Σ. This is simply Green's third identity applied to the region $\Omega \setminus \Sigma$. It is straightforward to check that since $\left[\frac{\partial u}{\partial \nu}\right]$ has at most an $r^{-1/2}$ singularity at the endpoints of any crack and since the singularity of Γ at $x = y$ is only logarithmic, equation (4.1) also holds for $x \in \Sigma$. Because u is a constant c_l on σ_l (and continuous in Ω) this implies that

$$\int_{\partial\Omega} (u(y)\frac{\partial}{\partial \nu_y}\Gamma(x,y) - \Gamma(x,y)\psi(y))\, ds_y - \sum_{k=1}^{n} \int_{\sigma_k} \Gamma(x,y)\phi_k(y)\, ds_y = c_l \tag{4.2}$$

for $x \in \sigma_l$. For $x \in \partial\Omega$, an argument similar to that which led to (4.1) leads to the equation

$$-\frac{1}{2}u(x) + \int_{\partial\Omega} u(y)\frac{\partial}{\partial \nu_y}\Gamma(x,y)\, ds_y - \sum_{k=1}^{n} \int_{\sigma_k} \Gamma(x,y)\phi_k(y)\, ds_y = \int_{\partial\Omega} \Gamma(x,y)\psi(y)\, ds_y. \tag{4.3}$$

As discussed earlier, if the constants c_l are treated as unknowns they can be determined uniquely from

$$\int_{\sigma_l} \phi_l\, ds = 0, \quad l = 1, \ldots n, \tag{4.4}$$

with the normalization $\int_{\partial\Omega} u\, ds = 0$. Combining these $n+1$ conditions with equations (4.2) and (4.3) we arrive at the following system of integral equations

$$\begin{aligned} -\frac{1}{2}u(x) + \int_{\partial\Omega} u(y)\frac{\partial}{\partial \nu_y}\Gamma(x,y)\, ds_y \;&-\; \sum_{k=1}^{n} \int_{\sigma_k} \Gamma(x,y)\phi_k(y)\, ds_y \\ &= \int_{\partial\Omega} \Gamma(x,y)\psi(y)\, ds_y, \quad x \in \partial\Omega \end{aligned} \tag{4.5}$$

$$\begin{aligned} \int_{\partial\Omega} u(y)\frac{\partial}{\partial \nu_y}\Gamma(x,y)\, ds_y \;&-\; \sum_{k=1}^{n} \int_{\sigma_k} \Gamma(x,y)\phi_k(y)\, ds_y - c_l \\ &= \int_{\partial\Omega} \Gamma(x,y)\psi(y)\, ds_y, \quad x \in \sigma_l \end{aligned} \tag{4.6}$$

with the additional constraints

$$\begin{aligned} \int_{\sigma_l} \phi_l\, ds &= 0, \quad l = 1, \ldots n, \\ \int_{\partial\Omega} u\, ds &= 0. \end{aligned} \tag{4.7}$$

The unknowns here are the value of u on $\partial\Omega$, ϕ_k on σ_k and the constants c_l, $l = 1, \ldots, n$. Given a set of cracks Σ and Neumann data ψ one can solve equations (4.5), (4.6) and (4.7)

to obtain these quantities. The solution to the boundary value problem (3.2) at any point in Ω can then be obtained from the representation (4.1).

One useful fact to note is the following. Let u_0 be a harmonic function on Ω with Neumann data ψ. The same reasoning used to derive the integral equations for u shows that u_0 satisfies the boundary integral equation

$$-\frac{1}{2}u_0(x) + \int_{\partial\Omega} u_0(y)\frac{\partial}{\partial\nu_y}\Gamma(x,y)\,ds_y = \int_{\partial\Omega}\Gamma(x,y)\psi(y)\,ds_y \tag{4.8}$$

for $x \in \partial\Omega$. A unique solution again requires a normalization such as $\int_{\partial\Omega} u_0\,ds = 0$. If $x \in \Omega$ then $u_0(x)$ can be represented

$$u_0(x) = \int_{\partial\Omega}(u_0(y)\frac{\partial}{\partial\nu_y}\Gamma(x,y) - \Gamma(x,y)\psi(y))\,ds_y. \tag{4.9}$$

Let v denote the difference $u - u_0$. Combining equation (4.5) with (4.8) and combining (4.6) with equation (4.9), we find that v satisfies

$$\begin{aligned} -\frac{1}{2}v(x) + \int_{\partial\Omega} v(y)\frac{\partial}{\partial\nu_y}\Gamma(x,y)\,ds_y - \sum_{k=1}^{n}\int_{\sigma_k}\Gamma(x,y)\phi_k(y)\,ds_y &= 0, \quad x \in \partial\Omega \qquad (4.10)\\ \int_{\partial\Omega} v(y)\frac{\partial}{\partial\nu_y}\Gamma(x,y)\,ds_y - \sum_{k=1}^{n}\int_{\sigma_k}\Gamma(x,y)\phi_k(y)\,ds_y - c_l &= -u_0(x), \quad x \in \sigma_l \end{aligned}$$

where ϕ_k denotes the jump in the normal derivative $\frac{\partial}{\partial\nu}v$ across σ_k. Note that this is the same as the jump in $\frac{\partial}{\partial\nu}u$, since u_0 is smooth in Ω. The conditions

$$\begin{aligned} \int_{\sigma_l}\phi_l\,ds &= 0, \quad l = 1,\ldots n, \qquad (4.11)\\ \int_{\partial\Omega} v\,ds &= 0, \end{aligned}$$

are also still enforced. Equations (4.10) and (4.11) provide a means of directly computing the perturbation $v = u - u_0$ caused by the presence of the cracks. This formulation is more advantageous than the original formulation since we will use singular boundary data ψ. The function $v = u - u_0$, however, is smooth up to $\partial\Omega$ and hence avoids any of the problems associated with the lack of regularity of ψ. Moreover, for the specific two-electrode Neumann data (and a domain in the form of a ball, as considered later) we have a closed form solution for u_0.

Having derived the boundary integral formulation we now briefly discuss how we discretize it by means of the so-called Nyström method. Suppose that the boundary of the region Ω

is parameterized by $z(t) = (z_1(t), z_2(t))$, $0 \le t < 1$. Let each crack σ_k be parameterized by $z(t)$ for $k \le t < k+1$. In terms of this parameterization, equations (4.10) and (4.11) can be written as

$$\begin{aligned} -\frac{1}{2}\phi(s) + \int_0^1 K(s,t)\phi(t)\,dt - \sum_{k=1}^{n}\int_k^{k+1} G(s,t)\phi(t)\,dt &= 0, \ s \in [0,1) \\ \int_0^1 K(s,t)\phi(t)\,dt - \sum_{k=1}^{n}\int_k^{k+1} G(s,t)\phi(t)\,dt - c_l &= -u_0(z(s)), \ s \in [l, l+1) \end{aligned} \tag{4.12}$$

and

$$\begin{aligned} \int_l^{l+1} \phi(t)|z'(t)|\,dt &= 0, \quad l = 1, \ldots, n, \\ \int_0^1 \phi(t)|z'(t)|\,dt &= 0 \end{aligned}$$

where $K(s,t) = \frac{\partial}{\partial \nu_y}\Gamma(z(s), z(t))|z'(t)|$ and $G(s,t) = \Gamma(z(s), z(t))|z'(t)|$. The functions v and ϕ_k have also been replaced by the single function ϕ defined on $[0, n+1]$ by $\phi(t) = v(z(t))$ for $t \in [0,1)$, $\phi(t) = \phi_k(z(t)$ for $t \in [k, k+1)$.

Let t_j and ω_j, $j = 1, \ldots, m$, denote the nodes and weights of a quadrature rule on $[0,1]$, so that

$$\int_0^1 f(t)\,dt \approx \sum_{j=1}^{m} \omega_j f(t_j)$$

for reasonably smooth functions $f(t)$. *Nyström's* method for solving an integral equation of the form

$$\phi(s) + \int_0^1 K(s,t)\phi(t)\,dt = f(s)$$

consists of replacing the integral by a quadrature rule to obtain

$$\tilde{\phi}(s) + \sum_{j=1}^{m} K(s,t_j)\omega_j\tilde{\phi}(t_j) = f(s).$$

Letting s assume the values $t_1, \ldots, t_m$ we obtain the $m \times m$ linear system

$$\phi_i + \sum_{j=1}^{m} K_{ij}\phi_j = f_i \quad i = 1, \ldots, m$$

where $\phi_i = \tilde{\phi}(t_i)$, $K_{ij} = K(t_i, t_j)\omega_j$ and $f_i = f(t_i)$. The intention is that $\phi_i = \tilde{\phi}(t_i) \approx \phi(t_i)$. A complete treatment of Nyström's method for second kind Fredholm equations can be found in [2].

For a first kind integral equation with a smooth kernel,

$$T_K\phi \equiv \int_0^1 K(s,t)\phi(t)\,dt = f(s),$$

direct discretization usually leads to a linear system which is very poorly conditioned. This stems from the fact that the corresponding inverse operator T_K^{-1} is unbounded on whatever space the equation is posed, typically $C(0,1)$ or $L^2(0,1)$. The singular values of the operator T_K approach zero rapidly, so that the solution ϕ is extremely sensitive with respect to f or to noise on the right hand side of the equation. The smoother the kernel, the faster the singular values decay and the poorer is the conditioning of the linear system. The solution of first kind integral equations therefore often requires some kind of regularization. As discussed in [5], however, if the kernel $K(s,t)$ is singular enough on the diagonal $s = t$, reasonable results can be obtained from a direct discretization of the equation, without regularization. In the case of equations (4.12) the first kind portion of the equations (on the cracks) have a logarithmic singularity along the diagonal $s = t$, and hence regularization should not be necessary. We have applied Nyström's method directly to the equations. The linear systems obtained in this manner have good conditioning and in all test cases in which we have a closed form solution, this method has produced solutions in complete agreement with the closed form solution.

To apply Nyström's method to the equations (4.12), we replace the integrals over the intervals $[l, l+1]$, $l = 0,\ldots,n$, with the quadrature rule and then let s assume the values $l + t_i$, $i = 1,\ldots,m$, $l = 0,\ldots,n$. This yields the following linear system in the variables $\phi_{01},\ldots,\phi_{0m},\phi_{11},\ldots,\phi_{nm},\tilde{c}_1,\ldots,\tilde{c}_n$:

$$\begin{aligned} -\frac{1}{2}\phi_{0i} + \sum_{j=1}^{m} K(t_i,t_j)\omega_j\phi_{0j} - \sum_{k=1}^{n}\sum_{j=1}^{m} G(t_i,k+t_j)\omega_j\phi_{kj} &= 0, \qquad (4.13)\\ i &= 1,\ldots,m \\ \sum_{j=1}^{m} K(l+t_i,t_j)\omega_j\phi_{0j} - \sum_{k=1}^{n}\sum_{j=1}^{m} G(l+t_i,k+t_j)\omega_j\phi_{kj} - \tilde{c}_l &= -u_0(z(l+t_i)), \\ i = 1,\ldots,m,\ \ l &= 1,\ldots,n \end{aligned}$$

and

$$\sum_{j=1}^{m} \phi_{lj}\omega_j |z'(l+t_j)| = 0, \quad l = 1,\ldots,n,$$

$$\sum_{j=1}^{m} \phi_{0j}\omega_j |z'(t_j)| = 0,$$

where the intention is that $\phi_{kj} \approx \phi(k+t_j)$ and $\tilde{c}_k \approx c_k$. In this formulation there are actually $mn+m+n+1$ equations for the $mn+m+n$ unknowns ϕ_{kj}, $k = 0,\ldots,n$, $j = 1,\ldots,m$ and $\tilde{c}_k$, $k = 1,\ldots n$. However, a careful analysis shows that the first m equations have a linear dependency (the coefficients sum to zero) so that any one of them, e.g., the first, can be dropped. This gives a linear system of $mn+m+n$ equations for the unknowns ϕ_{kj} and $\tilde{c}_k$.

One need not use the same quadrature rule on the boundary of Ω and the cracks. Since the solution is smooth on $\partial\Omega$, we allocate evenly spaced nodes there by $t_i = i/m$, $i = 0,\ldots,m-1$. The weights are simply $\omega_i = 1/m$, corresponding to the trapezoidal rule on the closed curve $\partial\Omega$. On each crack ϕ will typically have $r^{-1/2}$ singularities at the endpoints and so a quadrature rule is chosen which places more nodes near these singularities (but not actually at the endpoints). If the linear crack with endpoint at (a,b), angle θ and length λ is parameterized as $(a+t\lambda\cos\theta, b+t\lambda\sin\theta)$, $0 \le t < 1$, then the nodes are chosen as (assuming m is even)

$$t_i = f(\frac{i-1/2}{m}), \quad i = 1,\ldots,\frac{m}{2},$$

and $t_i = 1 - t_{m-i+1}$ for $i = \frac{m}{2}+1,\ldots,m$, where $f(x) = 2^{q-1}x^q$ and q is a positive number. The parameter q controls the spacing of the nodes with $q > 1$ causing the nodes to "bunch up" near 0 and 1. We have used $q = 2.5$. The weights ω_i are chosen as

$$\omega_i = \begin{cases} \frac{1}{2}(t_1+t_2), & i = 1 \\ \frac{1}{2}(t_{i+1}-t_{i-1}), & i = 2,\ldots,m-1 \\ 1-\frac{1}{2}(t_{m-1}+t_m), & i = m \end{cases}$$

corresponding to a midpoint rule with variably spaced nodes. We have used 60 nodes on both $\partial\Omega$ and each crack.

One difficulty with discretizing equations (4.12) is the presence of the logarithmic singularity in the first kind portion of the equations along the diagonal $s = t$. We deal with this

by using a simple form of product integration based on our quadrature rule. See [2], Section 3.2, for more details.

5 The Jacobian and Newton's Method

We recall that a central part of our crack reconstruction algorithm is to find a solution of the $4n \times 4n$ system

$$\begin{aligned} \mathbf{G}_k(\Sigma) &= \mathbf{F}(\Sigma, \psi_{\sigma_k}, \mathbf{w}_{\sigma_k}) - \mathbf{F}(\Sigma^*, \psi_{\sigma_k}, \mathbf{w}_{\sigma_k}) \\ &= \mathbf{F}(\Sigma, \psi_{\sigma_k}, \mathbf{w}_{\sigma_k}) - \mathbf{f}\ (\psi_{\sigma_k}, \mathbf{w}_{\sigma_k}), \quad k = 1, \ldots, n. \end{aligned} \tag{5.1}$$

Here the four components of $\mathbf{F}(\Sigma, \psi, \mathbf{w})$ are given by

$$F(\Sigma, \psi, w^{(i)}) = \int_{\partial\Omega} u(\Sigma, \psi) \frac{\partial w^{(i)}}{\partial \nu}\, ds \quad i = 1, \ldots, 4,$$

where u solves (3.2) and $w^{(i)}$ are the functions from (3.9)-(3.11). If we use the vector $Q \in \mathbb{R}^{4n}$ to describe the crack configuration Σ and we parameterize $\partial(\Omega \setminus \Sigma)$ as described in the last section, then the discretized version of each of these components becomes

$$\tilde{F}(Q, \psi, w) = \sum_{j=1}^{m} u_j \frac{\partial w}{\partial \nu}(t_j) |z'(t_j)| \omega_j \tag{5.2}$$

where t_j is the *jth* node for Nyström's method on $\partial\Omega$, ω_j is the corresponding weight. The variables u_j are given by $u_j = u_0(t_j) + \phi_{0j}$, where ϕ_{0j} form the first part of the solution to the system (4.13).

Our approximate method for the solution of (5.1) is a variation of Newton's method. For that we need an effective method for the calculation of the Jacobian. If q denotes one of the components of Q, differentiation of the expression (5.2) yields

$$\begin{aligned} \frac{\partial \tilde{F}}{\partial q} &= \sum_{j=1}^{m} \left(\frac{\partial u_j}{\partial q} \frac{\partial w}{\partial \nu}(t_j) + u_j \frac{\partial}{\partial q} \left(\frac{\partial w}{\partial \nu}(t_j) \right) \right) |z'(t_j)| \omega_j \\ &= \sum_{j=1}^{m} \left(\frac{\partial \phi_{0j}}{\partial q} \frac{\partial w}{\partial \nu}(t_j) + (u_0(t_j) + \phi_{0j}) \frac{\partial}{\partial q} \left(\frac{\partial w}{\partial \nu}(t_j) \right) \right) |z'(t_j)| \omega_j. \end{aligned} \tag{5.3}$$

Here we have assumed that $|z'|$ is independent of q on $\partial\Omega$ and, as mentioned previously, we have ignored the functional dependence of the applied current flux ψ on Σ (this in

particular gives that $\frac{\partial u_0}{\partial q} = 0$). Note that the functions w defined by (3.9)- (3.11) are indeed differentiable with respect to the parameters describing the cracks.

To evaluate $\frac{\partial \tilde{F}}{\partial q}$ from equation (5.3) we therefore need to calculate $\frac{\partial \phi}{\partial q}$, the derivatives of the solution to (4.13) with respect to the parameters which describe the cracks. These can be computed with little additional effort. Let the linear system (4.13) be written in the form

$$A(Q)\phi(Q) = f(Q) \tag{5.4}$$

where $A(Q)$ is the $mn+m+n$ by $mn+m+n$ matrix appearing in (4.13), $f(Q) \in \mathbb{R}^{mn+m+n}$ is the right hand side, and $\phi(Q) \in \mathbb{R}^{mn+m+n}$ is the solution to the system (including the constants c). Of course all of these quantities depend on the parameters Q. Differentiation of equation (5.4) with respect to any one of the parameters of Q and use of the fact that $\frac{\partial u_0}{\partial q} = 0$ gives

$$A(Q)\frac{\partial \phi}{\partial q} = \frac{\partial f}{\partial q} - \frac{\partial A}{\partial q}\phi(Q) = -\frac{\partial A}{\partial q}\phi(Q), \tag{5.5}$$

so the derivative satisfies a linear equation of exactly the same form as ϕ but with a different right hand side. Once (5.4) has been solved for $\phi(Q)$ (e.g., by LU decomposition), equation (5.5) can be solved for $\frac{\partial \phi}{\partial q}$ by simply computing the right hand side and reusing the LU decomposition.

Below is a global description of our algorithm for crack reconstruction. We denote by $\Sigma^i = \{\sigma_j^i\}_{k=1}^n$ the estimated cracks at the *ith* stage of the algorithm, and by Q^i we denote the corresponding set of parameters.

1. Make an initial guess Σ^0, set $i = 0$.

2. Select the maximally sensitive two-electrode fluxes $\psi_{\sigma_k^i}$ corresponding to the cracks σ_k^i, $k = 1, \ldots, n$, in the sense defined in section 3.

3. Measure (simulate) the boundary voltage data for each flux and compute $\mathbf{f}(\psi_{\sigma_k^i}, \mathbf{w}_{\sigma_k^i})$, $k = 1, \ldots, n$.

4. Compute the voltage data for each flux at $\Sigma = \Sigma^i$ and compute $\mathbf{F}(\Sigma^i, \psi_{\sigma_k^i}, \mathbf{w}_{\sigma_k^i})$, $k = 1, \ldots, n$.

5. Compute $G_k(\Sigma^i) = \mathbf{F}(\Sigma^i, \psi_{\sigma_k^i}, \mathbf{w}_{\sigma_k^i}) - \mathbf{f}(\psi_{\sigma_k^i}, \mathbf{w}_{\sigma_k^i})$, $k = 1, \ldots, n$. Let $G(\Sigma)$ denote the vector of all residuals$\{G_k(\Sigma)\}_{k=1}^n$ (a $4n$-vector). If $G(\Sigma^i)$ $(= G(Q^i))$ is sufficiently small, terminate with the answer $\Sigma = \Sigma^i$.

6. Compute the approximate Jacobian $J_i =$ "$D_Q G(Q)|_{Q=Q^i}$", in the sense described earlier.

7. Compute the Newton update δQ^i by solving $J_i \delta Q^i = -G(Q^i)$.

8. Update $Q^{i+1} = Q^i + \delta Q^i$, $i = i + 1$, and go to step 2.

In our implementation of Newton's method, as in [15], we solve the linear system

$$J_i \delta Q^i = -G(Q^i)$$

subject to the constraint

$$\|A(\delta Q^i)\| \leq \rho$$

where A is an appropriately chosen diagonal weighting matrix and ρ a specified parameter. This constrained problem is solved in the least squares sense by means of a Lagrange multiplier method as outlined in [11]. The constraint on the update markedly improves the behavior of Newton's method far from the solution.

It should be mentioned that we also constrain the cracks to lie inside the domain Ω; if the algorithm attempts to move a crack outside Ω we perform a simple reflection of the endpoint(s) that lie outside to get get the updated crack fully inside Ω. The algorithm very rarely attempts to move a crack outside the domain (unless the data based on which we perform the reconstruction is generated from a collection of cracks, at least which of one lies very near the boundary). Our implementation will also allow the cracks to intersect each other; the integral equation formulation continues to make sense in this case, although in practice one must be careful when dealing with the logarithmic singularities which arise as a result of the intersection. We deal with this by again using a form of product integration.

6 Computational Experiments

We have performed a significant amount of computational experimentation with the algorithm we have developed. In this section we briefly describe five such experiments which we find to be representative. The experiments are all performed on simulated data. It is our goal to eventually try our algorithm on actual experimental data. A project to build an experimental setup and a data gathering device is currently in progress [10]. To go part of the way towards reconstruction based on real data, the last of the experiments described here pertains to simulated data with a built-in level of noise.

The domain on which the reconstruction is performed is in all cases the unit disk. The graphics by means of which we illustrate the progress of the algorithm is the same for all experiments. Each step in the iteration is illustrated by a picture containing two copies of the unit disk. The disk on the left depicts the previously estimated locations of the cracks (a set of line segments) as well as the boundary locations of the optimally sensitive electrode locations. The electrode locations are marked with small circles; the circle corresponding to P_0 has been darkened. It is voltage data corresponding to the currents generated by these electrode locations that are used for the iterative update. The updated estimates of the crack locations are shown as solid line segments in the disk on the right. The true cracks which the algorithm seeks to reconstruct, *i.e.*, the cracks from which the simulated boundary voltage data is generated, are shown as dashed line segments (or dashed circular arcs) in the disk on the right.

In our first experiment the simulated data comes from three cracks, two of which are very near the boundary. They are each 0.05 units away from the boundary. The cracks have lengths 0.25, 0.3 and 0.35. We start the reconstruction procedure by attempting to fit the simulated data with data generated from a single crack. As the initial guess we select a crack joining the points (-0.2, 0.2) to (-0.2, 0.6). Figure 1a shows the first step of the iteration. After 31 steps the algorithm has found a root for the system of four functionals and reduced the residual error ($|G(Q)|$) to 8.94×10^{-13}. Figure 1b shows step 31 of the iteration.

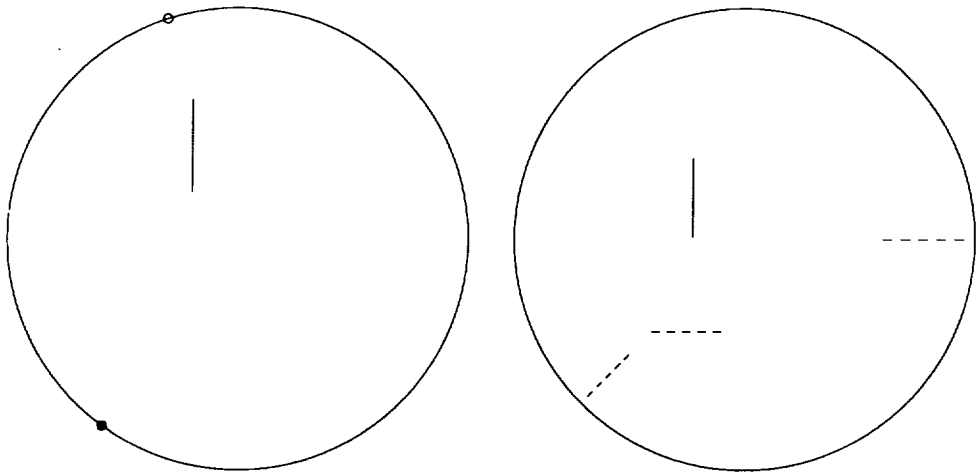

Figure 1a: Iteration 1: one crack fitted to three crack boundary data.

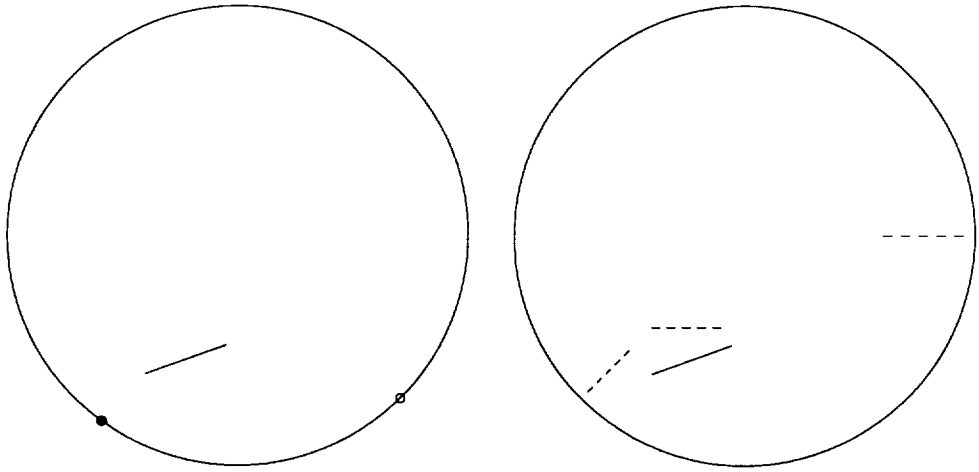

Figure 1b: Iteration 31: one crack fitted to three crack boundary data.

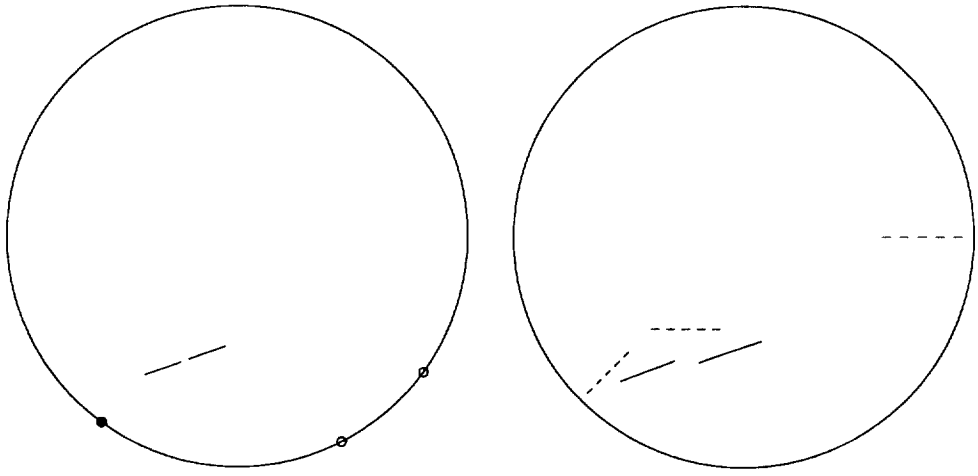

Figure 1c: Iteration 1: two cracks fitted to three crack boundary data.

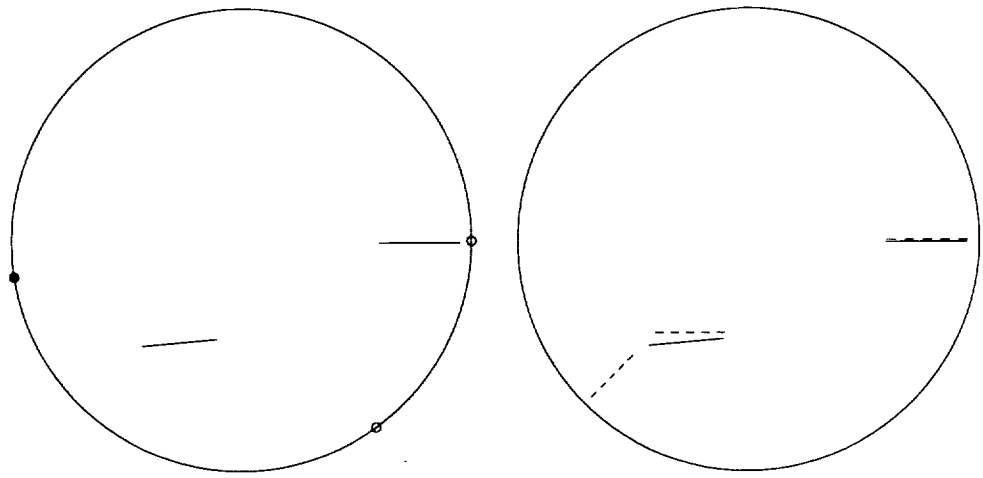

Figure 1d: Iteration 18: two cracks fitted to three crack boundary data.

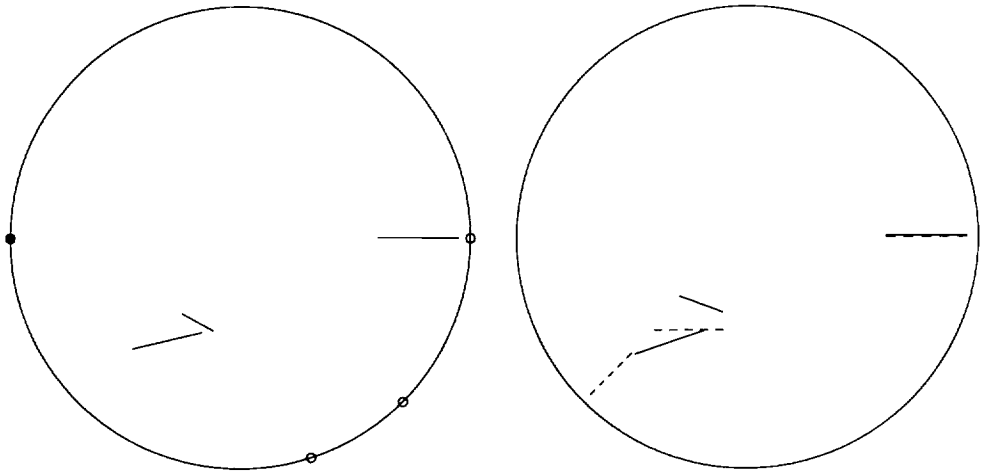

Figure 1e: Iteration 10: three cracks fitted to three crack boundary data.

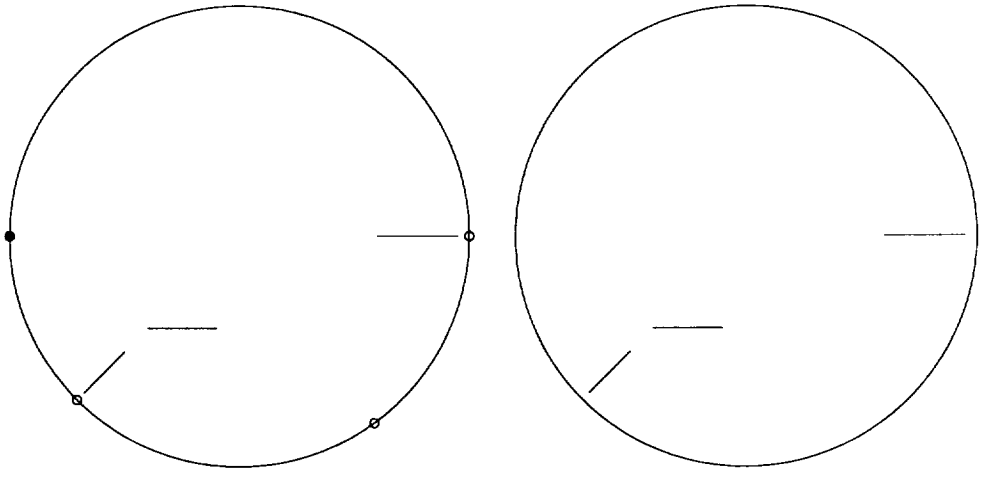

Figure 1f: Iteration 24: three cracks fitted to three crack boundary data.

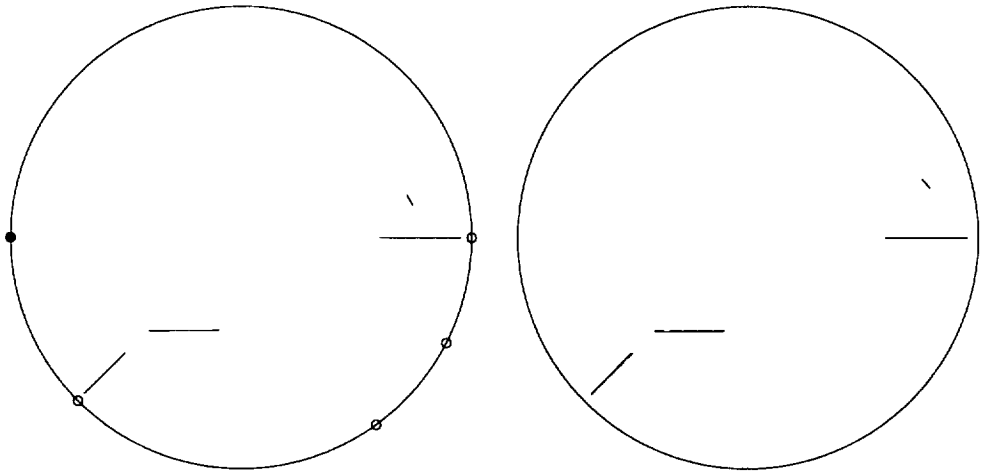

Figure 1g: Iteration 19: four cracks fitted to three crack boundary data.

At this point it is not possible, based on four functionals, to determine whether the simulated boundary voltage data comes from just a single crack or several more. The only way to determine this is to try to fit more functionals. We take the crack shown in the right disk in Figure 1b and divide it into two cracks by cutting out a piece 1/10 of the length at the center. The two resulting cracks are now used as the initial guess for our algorithm based on 8 functionals. The first step of the two-crack iteration is show in Figure 1c. After 18 steps the "two-crack iteration" has found a root to the 8-variable system and has reduced the residual error to 6.9×10^{-16}. The final step is shown in Figure 1d. Finally we take the largest of the two cracks from the right disk in Figure 1d, divide it into two pieces (by cutting out the middle 1/10), and give the resulting three cracks as initial guess to our algorithm based on 12 functionals. This "three crack iteration" locates the root after 24 steps, reducing the residual error to 2.0×10^{-11}. Steps 10 and 24 of this iteration are shown in Figure 1e and Figure 1f, respectively. If at this point we take and divide one of the three cracks again and give the resulting four cracks as an initial guess to our algorithm based on 16 functionals, then one of two things is likely to happen: 1) these new four crack will remain essentially where the three cracks already are (and the residual will be very small) 2) the algorithm will shrink one of the cracks to zero length and the three remaining will stay as before. In the latter case the residual will not become quite as small since we impose a lower limit (of 0.01) on the length of the cracks. In both cases the behavior clearly indicates that three cracks are the right number to fit the data (also for 16 functionals). Figure 1g shows step 19 in a

"four crack iteration" where the largest crack in Figure 1f has been divided into two pieces. As is evident the latter of the two possibilities from before emerges (the residual after 19 steps is 5.2×10^{-4}).

The strategy for gradually increasing the number of cracks as outlined above has emerged after a significant amount of numerical experimentation with many sets of simulated data. The alternate strategy: to initially guess a sufficient number of cracks and then let the iterations proceed to convergence has generally shown itself to lead to much slower convergence. Our method based on the use of only a few functionals and the adaptive movement of electrodes has in many of our experiments proven itself to be superior to a least squares fitting algorithm (using the entire set of boundary voltage data, but a fixed set of electrodes). Our experience with this least squares approach has been that, except for the one crack case, it requires a very accurate initial guess in order to converge to the correct solution. For multiple cracks the least squares functional appears to contain many local minima.

This is not to say that our approach may not occasionally be somewhat slower than indicated by the previous example. We illustrate this with a reconstruction based on simulated data from four cracks. Figure 2a shows the first step using a single crack (four functionals). After 17 steps our algorithm finds a root with the residual reduced to 1.72×10^{-14}. However, as seen in Figure 2b (which shows the final iteration) the single crack that is consistent with the four functionals does not lie near any of the four cracks that were used to generate the data. We now divide this single crack into two by cutting out the middle 1/10. Using the resulting two cracks as initial guess our algorithm based on 8 functionals now takes a considerable number of steps before the residual is even reasonably small (and the cracks are of reasonable size). Figures 2c and 2d show iterations 99 and 198, respectively. We take the two cracks after 198 iterations and divide each of them into two using the same method as before. The resulting four cracks are provided as initial guess for our algorithm based on 16 functionals. Iterations 50 and 115 of this process are shown in Figures 2e and 2f, respectively. After 127 iterations a root is found and the residual has been reduced to 1.65×10^{-14}. Even though the algorithm is extremely slow it does ultimately converge. It would require an extremely accurate initial guess to get the least squares algorithm we described before to converge. For comparison figure 2g shows the eleventh and final

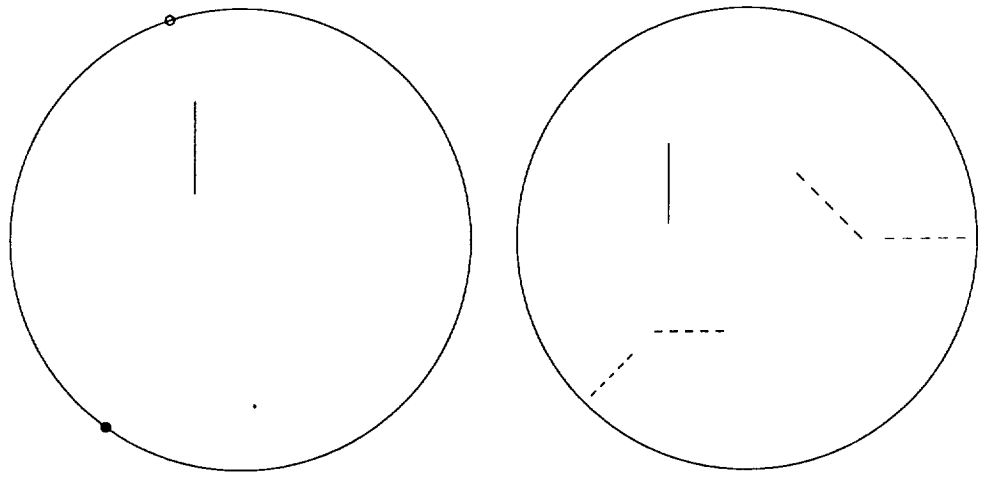

Figure 2a: Iteration 1: one crack fitted to four crack boundary data.

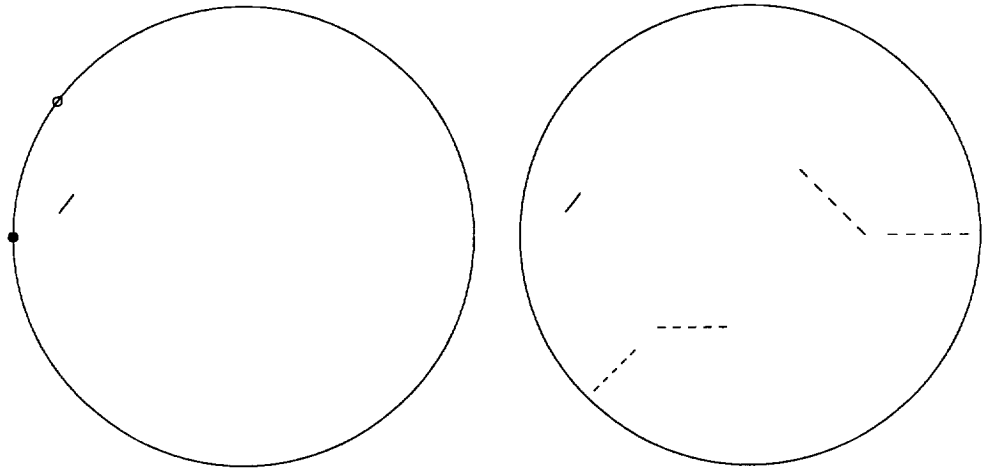

Figure 2b: Iteration 17: one crack fitted to four crack boundary data.

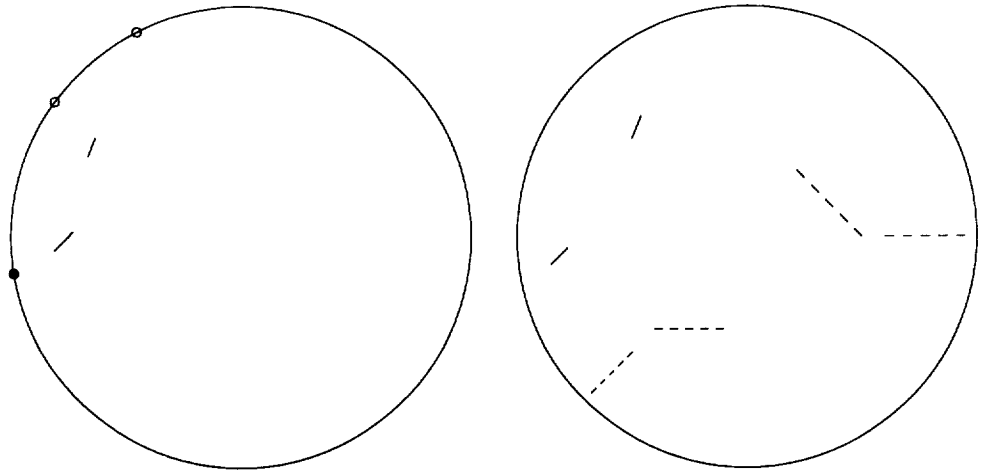

Figure 2c: Iteration 99: two cracks fitted to four crack boundary data.

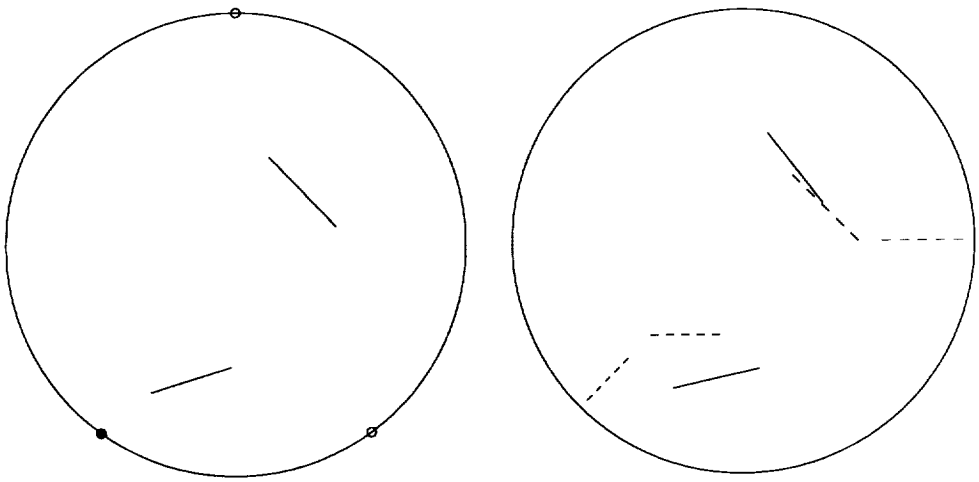

Figure 2d: Iteration 198: two cracks fitted to four crack boundary data.

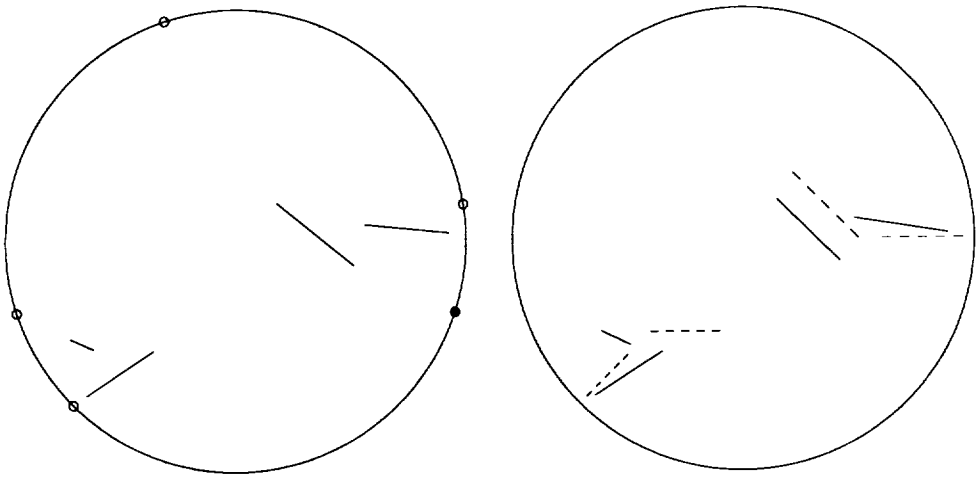

Figure 2e: Iteration 50: four cracks fitted to four crack boundary data.

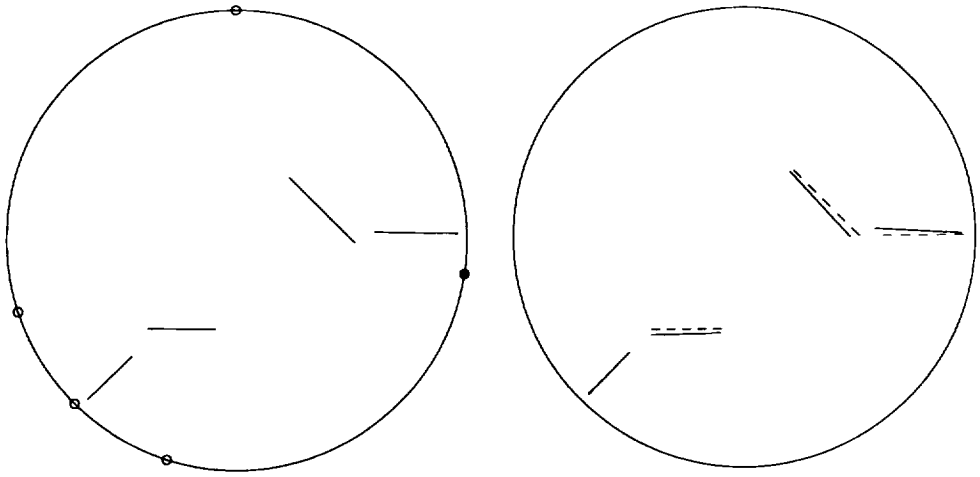

Figure 2f: Iteration 115: four cracks fitted to four crack boundary data.

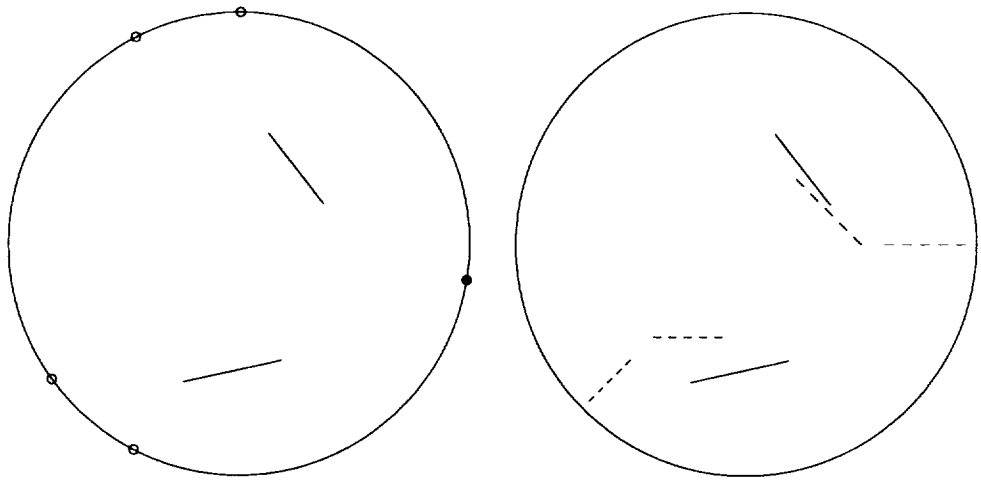

Figure 2g: Least squares, iteration 11: four cracks fitted to four crack data.

iterate of a least squares approach. This computation was done using the full boundary data and a Levenberg-Marquardt algorithm as outline in [11]. The initial guess used (consisting of four cracks) is the same as that used for figures 2e and 2f. The least squares approach quickly locates a local minimum and terminates. The four cracks that are used appear to merge into two.

Frequently in practice there are either a fairly limited number of well-separated cracks, or many cracks clustered in certain locations. Figures 3a and 3b show the first iteration and the fifth iteration using our algorithm with one crack (and four functionals) to fit simulated data coming from 10 cracks located in two clusters. A root is found at the fifth iteration

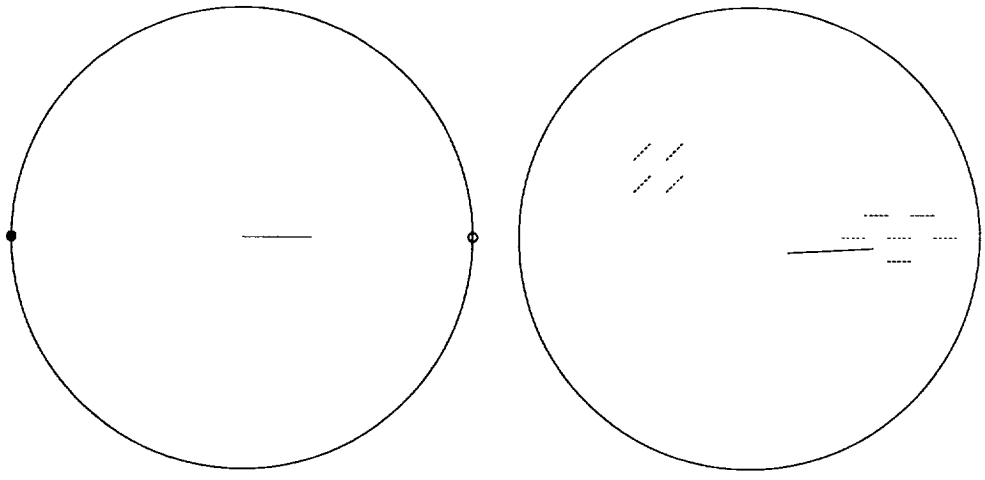

Figure 3a: Iteration 1: one crack fitted to ten crack boundary data.

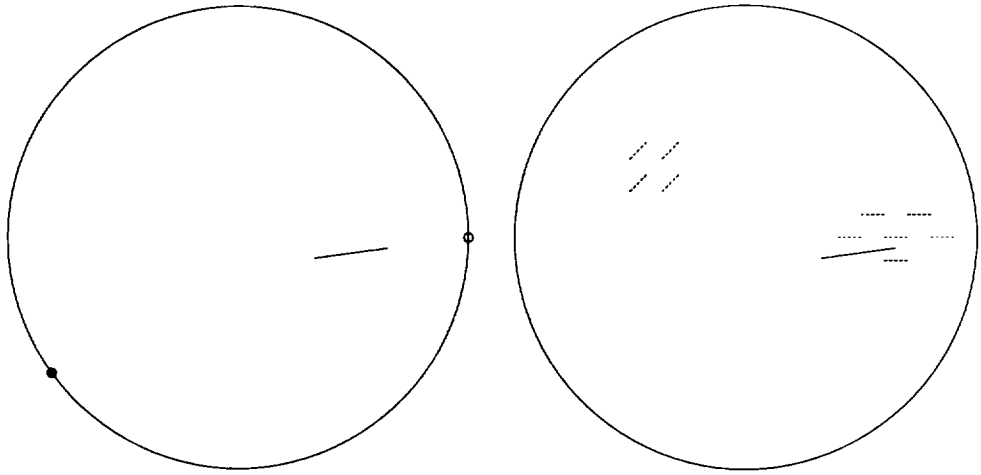

Figure 3b: Iteration 5: one crack fitted to ten crack boundary data.

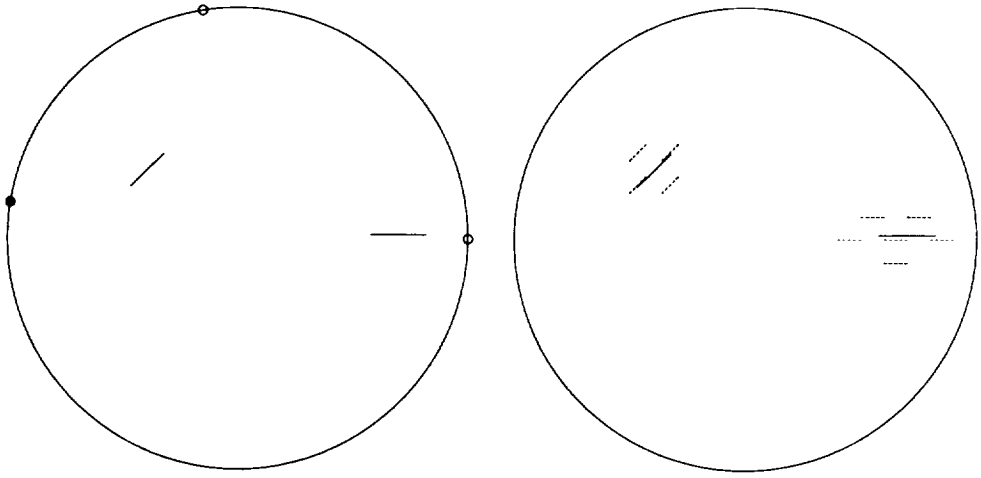

Figure 3c: Iteration 15: two cracks fitted to ten crack boundary data.

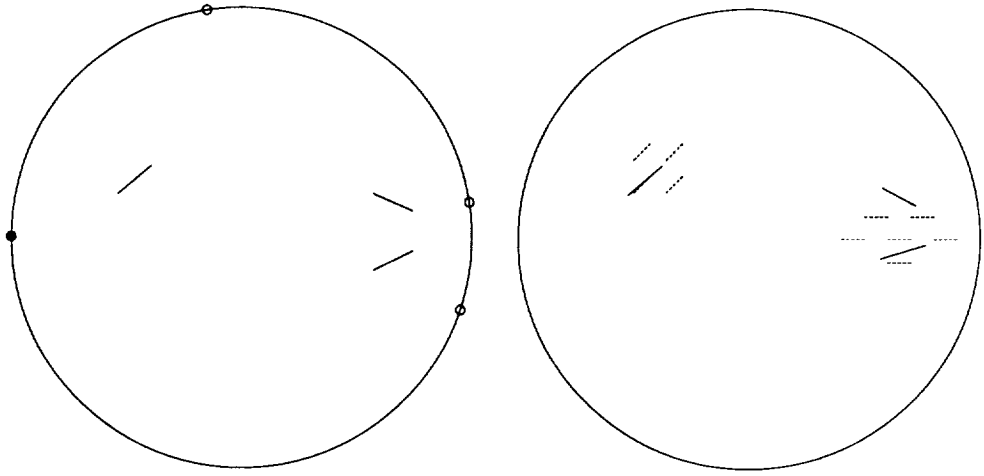

Figure 3d: Iteration 99: three cracks fitted to ten crack boundary data.

guess to the "four crack version" of our algorithm. Figure 4d shows iteration 50 using four cracks. The algorithm has not yet located a root. The two longest cracks, which already emerge after 13 iterations, provide a reasonable approximation to the curved crack. One of the two shorter cracks stays close to the circular arc (and the two large cracks) the other one seeks to exit the domain; the program apparently cannot adjust them to find a root, but there is a lower bound on their length, so they cannot entirely disappear.

In the final example we have taken data generated by a two cracks and added 10% noise. The noise added is independent and gaussian with a zero mean and standard deviation equal to 1/10 the mean square value of $u - u_0$ on $\partial\Omega$, where u is the potential

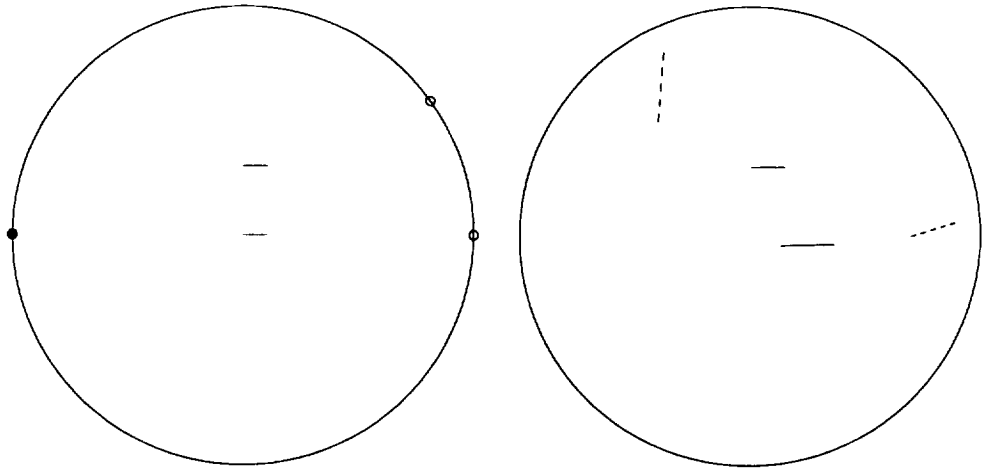

Figure 5a: Iteration 1: two crack fitted to two crack data, 10 percent noise.

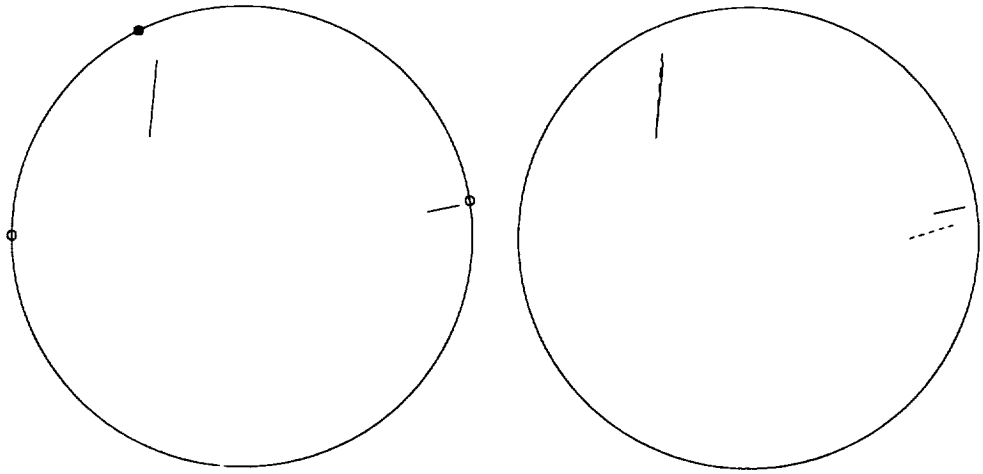

Figure 5b: Iteration 24: two crack fitted to two crack data, 10 percent noise.

and u_0 is the harmonic function with the same flux as u. In figure 5a we show the first iteration. Figure 5b shows the 24th iteration, at which point the algorithm terminates having found a root. Figure 5c shows the result of taking the final crack locations in figure 5b and using them as an initial guess to a least-squares minimization routine. This routine uses a fixed set of electrodes, those from the last iteration of our algorithm. These are presumably close to the most sensitive electrode locations for the given cracks. The Levenberg-Marquardt routine reduces the total least-squares residual from 0.085 to 0.032 in 13 iterations and improves the estimate of the crack locations.

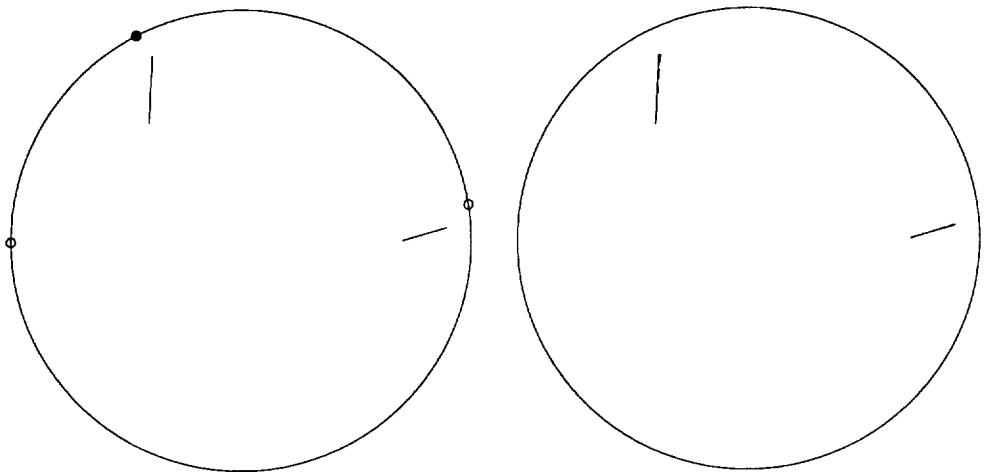

Figure 5c: Least squares, iteration 13: two crack fitted to two crack data, 10 percent noise.

7 Summary

In this paper we have developed a very efficient algorithm for the reconstruction of a collection of cracks based on electrostatic boundary measurements. We use a "dual" variational formulation for the forward electrostatic problem, and solve this numerically by means of a Nyström's approximation of the corresponding boundary integral equations. Our reconstruction is based on adaptively changing the current patterns, so as to maximize the sensitivity of the measured voltage differences. Our reconstruction is based on a limited set of averages of the boundary voltage measurements as opposed to the entire set of measurements; this should lead to greater efficiency and less rigidity. The algorithm is currently entirely

two-dimensional, but it should be very interesting to extend it to three dimensions. At this point we have only investigated the behavior of the algorithm when used on "synthetic" data (including data with noise). It should be very interesting to apply the algorithm to data coming from "real" experiments. Frequently cracks appear as clusters of many small (microscopic) cracks; our algorithm, when applied to data generated by clusters of small cracks, often very successfully locates a set consisting of a few, well-separated cracks. In this context it should be extremely interesting to analyze in what sense this reflects the behavior of the forward problem. To be more specific: it should be interesting to study in what sense a cluster of small (microscopic) cracks in an appropriate limit approaches a single (lumped) macroscopic crack.

References

[1] Alessandrini, G., Stable determination of a crack from boundary measurements. To appear, Proc. Roy. Soc. Edinburgh.

[2] Atkinson, K.E., *A survey of numerical methods for the solution of fredholm integral equations of the second kind*, SIAM, Philadelphia, PA, 1976.

[3] Barber, D. and Brown, B., Recent developments in applied potential tomography - APT, in Information Processing in Medical Imaging, Bacharach, S. ed., Nijhoff, Amsterdam, 1986, pp. 106–121.

[4] Bryan, K. and Vogelius, M., A uniqueness result concerning the identification of a collection of cracks from finitely many electrostatic boundary measurements. To appear, SIAM J. Math. Anal.

[5] de Hoog, F.R., Review of fredholm equations of the first kind. In *the application and numerical solution of integral equations*, Andersen, R.S. et al (eds.), Sijthoff and Noordhoff: Alphen aan den Rijn, 1980.

[6] Eggleston, M.R., Schwabe, R.J., Isaacson, D., Goble, J.C. and Coffin, L.F., Three-dimensional defect imaging with electric current computed tomography. GE Technical Report 91CRD039, Schenectady, NY.

[7] Folland, G.B., *Introduction to partial differential equations.* Princeton, NJ: Princeton University Press, 1976.

[8] Friedman, A. and Vogelius, M., Determining cracks by boundary measurements. Indiana Univ. Math. J., 38 (1989), pp 527–556.

[9] Gisser, D.G., Isaacson, D. and Newell, J.C., Electric current computed tomography and eigenvalues. SIAM J. Appl. Math., 50 (1990), pp 1623–1634.

[10] Liepa, V., Santosa, F. and Vogelius, M. Crack determination from boundary measurements: Computational reconstruction from laboratory measurements. Submitted to Journal of Nondestructive Evaluation.

[11] Moré, J., The Levenberg-Marquardt algorithm: implementation and theory. *Numerical Analysis* (Edited by Watson, G.A.), pp. 105–116. *Lecture Notes in Math.* 630. Springer Verlag, 1977.

[12] Nedelec, J.C., Integral equations with non integrable kernels. Integral Eq. Operator Th., 5 (1982), pp 562–572.

[13] Nishimura, N., Regularized integral equations for crack shape determination problems. *Inverse Problems in Engineering Sciences* (Edited by Yamaguti, M. et al), pp. 59–65. Springer Verlag, 1991.

[14] Nishimura, N. and Kobayashi, S., A boundary integral equation method for an inverse problem related to crack detection. Int. J. Num. Meth. Eng., 32 (1991), pp 1371–1387.

[15] Santosa, F. and Vogelius, M., A computational algorithm to determine cracks from electrostatic boundary measurements. Int. J. Eng. Sci. 29 (1991), pp 917–937.

[16] Yorkey, T., Webster, J. and Tompkins, W., Comparing reconstruction algorithms for electrical impedance tomography. IEEE Trans. Biomedical Eng., BME-34 (1987), pp. 843–852.

REPORT DOCUMENTATION PAGE

Form Approved
OMB No. 0704-0188

1. AGENCY USE ONLY (Leave blank)	2. REPORT DATE	3. REPORT TYPE AND DATES COVERED
	June 1992	Contractor Report

4. TITLE AND SUBTITLE
A COMPUTATIONAL ALGORITHM FOR CRACK DETERMINATION. THE MULTIPLE CRACK CASE

5. FUNDING NUMBERS
C NAS1-18605
C NAS1-19480
WU 505-90-52-01

6. AUTHOR(S)
Kurt Bryan
Michael Vogelius

7. PERFORMING ORGANIZATION NAME(S) AND ADDRESS(ES)
Institute for Computer Applications in Science and Engineering
Mail Stop 132C, NASA Langley Research Center
Hampton, VA 23665-5225

8. PERFORMING ORGANIZATION REPORT NUMBER
ICASE Report No. 92-24

9. SPONSORING/MONITORING AGENCY NAME(S) AND ADDRESS(ES)
National Aeronautics and Space Adminstration
Langley Research Center
Hampton, VA 23665-5225

10. SPONSORING/MONITORING AGENCY REPORT NUMBER
NASA CR-189665
ICASE Report No. 92-24

11. SUPPLEMENTARY NOTES
Langley Technical Monitor: Michael F. Card
Final Report
Submitted to International Journal of Engineering Sciences

12a. DISTRIBUTION/AVAILABILITY STATEMENT
Unclassified - Unlimited

Subject Category 64

12b. DISTRIBUTION CODE

13. ABSTRACT *(Maximum 200 words)*

This paper develops an algorithm for recovering a collection a linear cracks in a homogeneous electrical conductor from boundary measurements of voltages induced by specified current fluxes. The technique is a variation of Newton's method and is based on taking weighted averages of the boundary data. The method also adaptively changes the applied current flux at each iteration to maintain maximum sensitivity to the estimated locations of the cracks.

14. SUBJECT TERMS
inverse problems; nondestructive evaluation; boundary integral equations

15. NUMBER OF PAGES
40

16. PRICE CODE
A03

17. SECURITY CLASSIFICATION OF REPORT	18. SECURITY CLASSIFICATION OF THIS PAGE	19. SECURITY CLASSIFICATION OF ABSTRACT	20. LIMITATION OF ABSTRACT
Unclassified	Unclassified		

NSN 7540-01-280-5500

Standard Form 298 (Rev 2-89)
Prescribed by ANSI Std Z39-18
298-102